Biogeosciences Discuss., doi:10.5194/bg-2017-104, 2017
Manuscript under review for journal Biogeosciences
Discussion started: 30 March 2017

Biogeosciences Discussions Open Access EGU

A novel acclimative biogeochemical model and its implementation to the southern North Sea

Onur Kerimoglu[1], Richard Hofmeister[1], Joeran Maerz[1,2], and Kai W. Wirtz[1]

[1]Institute of Coastal Research, Helmholtz-Zentrum Geesthacht, Geesthacht, Germany
[2](present) Max Planck Institute for Meteorology, Hamburg, Germany

Correspondence to: Onur Kerimoglu (kerimoglu.o@gmail.com)

Abstract. Ecosystem models often rely on heuristic descriptions of autotroph growth that fail to reproduce various stationary and dynamic states of phytoplankton cellular composition observed in laboratory experiments. Here, we present the integration of an advanced phytoplankton growth model within a coupled 3-dimensional physical-biogeochemical model, and the implementation of the model system to the Southern North Sea (SNS) defined on a relatively high resolution (∼ 1.5-4.5 km) curvilinear grid. The autotrophic growth model, recently introduced by Wirtz and Kerimoglu (2016), is built up on a set of novel concepts for the allocation of internal resources and operation of cellular metabolism. The coupled model system consists of the general estuarine transport model (GETM) as the hydrodynamical driver, a lower trophic level model and a simple sediment diagenesis model. We force the model system with realistic atmospheric and riverine fluxes, background turbidity caused by suspended particulate matter and open ocean boundary conditions. For a simulation for the period 2000-2010, we show that the model system satisfactorily reproduces the physical and biogeochemical states of the system, as inferred from comparisons against data from long-term monitoring stations, sparse measurements, continuous transects, and remote sensing data. In particular, the model shows high skill both in coastal and off shore waters, and captures the steep gradients in nutrient and chlorophyll concentrations observed prevalently across the coastal transition zone. We show that the cellular chlorophyll to carbon ratio show significant seasonal and lateral variability, the latter amplifying the steepness of the transitional chlorophyll gradient, thus, pointing to the relevance of resolving the physiological acclimation processes for an accurate description of biogeochemical fluxes.

Wirtz, K.W. and Kerimoglu, O.: Optimality and variable co-limitation controls autotrophic stoichiometry, Frontiers in Ecology and Evolution, doi:10.3389/fevo.2016.00131, 2016.

1 Introduction

Modelling the biogeochemistry of coastal and shelf systems requires the representation of a multitude of interacting processes, not only within the water but also at the adjacent earth system components such as the atmosphere (e.g., nitrogen deposition), land (e.g., rivers), sediment (e.g., diagenetic processes), and biochemical processes in water (see., e.g., Cloern et al., 2014; Emeis et al., 2015). For being able to reproduce the large scale spatial and temporal distribution of biogeochemical variables in coastal systems, a realistic representation of hydrodynamical processes is often critically important, at least those relevant to

Biogeosciences Discuss., doi:10.5194/bg-2017-104, 2017
Manuscript under review for journal Biogeosciences
Discussion started: 30 March 2017

the circulation patterns and stratification dynamics: the former is needed to describe the spread of nutrient-rich river plumes and exchange at the open ocean boundaries, and the latter for being able to capture the vertical gradients in the light and nutrient conditions for primary productivity. Representation of biological processes and the two way interactions between biological, chemical and benthic compartments in models are particularly challenging, given the complexity of physiological processes displayed by individual organisms, e.g., regarding the regulation of their internal stoichiometries (e.g., see Bonachela et al., 2016) and the differences in functional traits of species constituting communities (e.g., see Litchman et al., 2010).

3-D ecosytem models often describe the processes relevant to primary production, e.g., the nutrient and light limitation of phytoplankton, using heuristic formulations that have been shown to be inadequate in reproducing patterns obtained in laboratory experiments. For instance, light limitation is determined not only by the instantaneously available irradiance, but also the amount of light harvesting apparatus, i.e., chlorophyll pigments maintained by the phytoplankton cells, through a process referred to as photoacclimation. However, photoacclimation is often completely ignored in 3-D model applications, or its effects are mimicked heuristically, for instance, by describing the chlorophyll to carbon ratio as a function of irradiance (Blackford et al., 2004; Fennel et al., 2006), which cannot capture the dependence of chlorophyll synthesis on nutrient availability (e.g., Pahlow and Oschlies, 2009; Smith et al., 2011). Similarly, interaction of limitation by different nutrient elements is described by heuristic formulations, dichotomously either by a product rule or a threshold function, which, again, cannot reproduce complex patterns observed in laboratory conditions, such as the asymmetric cellular N:C and P:C ratios emerging under N- and P-limited conditions (Bonachela et al., 2016; Wirtz and Kerimoglu, 2016). Such simplifications in the description of primary production processes, in turn, potentially lead to flawed representations of nutrient cycling. Despite the recently revived theoretical work on stoichiometric regulation and photoacclimation (e.g., Klausmeier et al., 2004; Pahlow and Oschlies, 2009; Wirtz and Pahlow, 2010; Bonachela et al., 2013; Daines et al., 2014), an implementation of a model with a mechanistic description of the regulation of phytoplankton composition at a full ecosystem scale in a coupled physical-biological modeling framework remains to be lacking. In this study, we present a 3-D application of the Model for Adaptive Ecosytems for Coastal Seas (hereafter MAECS), to the Southern North Sea (SNS), for a decadal hindcast simulation. MAECS features an photoacclimative autotrophic growth model that has been recently introduced by Wirtz and Kerimoglu (2016), which resolves the regulation of the stoichiometry and composition of autotrophs employing an innovative suit of adaptive and optimality based approaches.

SNS is part of a shallow shelf system (Fig.1). Especially the south eastern portion of the SNS, known as the German Bight surrounded by the inter-tidal Wadden Sea, is characterized by steep gradients with respect to both nutrients (Hydes et al., 1999; Ebenhöh, 2004) and turbidity. The latter is largely determined by suspended particulate matter (SPM) concentrations (Tian et al., 2009; Su et al., 2015). These gradients are driven by a complex interplay of riverine and atmospheric fluxes, complex topography, residual tidal currents, density gradients, biological processing of organic matter, benthic-pelagic coupling and sedimentation/resuspension dynamics (Postma, 1961; Puls et al., 1997; van Beusekom and de Jonge, 2002; Burchard et al., 2008; Hofmeister et al., 2016). A number of modelling studies previously addressed the biogeochemistry of the North Sea, including the German Bight. In a majority of these studies, such as ECOHAM-HAMSOM (Pätsch and Kühn, 2008), ECOSMO-HAMSOM (Daewel and Schrum, 2013), ERSEM-NEMO (de Mora et al., 2013; Ford et al., 2016), ERSEM-BFM-GETM (van Leeuwen et al., 2015; Ford et al., 2016) and HAMOCC-MPIOM (Gröger et al., 2013), large domains and relatively

Biogeosciences Discuss., doi:10.5194/bg-2017-104, 2017
Manuscript under review for journal Biogeosciences
Discussion started: 30 March 2017

coarse grids were employed ($\geq$ 7 km). While showing good skill in reproducing off-shore dynamics, these models seemed to have a relatively limited performance at the shallow, near-coast regions (when reported). The BLOOM-Delft3D (Los et al., 2008) on the other hand, is one of the rare examples with a finer grid (down to 1 km at the Dutch coasts) at the cost of a relatively smaller domain, similar to ours. Although this model system performs decently at both coastal and off-shore areas, its performance within the German Bight has not been fully assessed. Moreover, none of these models provide elaborate descriptions of the stoichiometric regulation of autotrophs, as mentioned above. Therefore, our new model system is expected to fill two important gaps by; 1) exemplifying for the first time to the best of our knowledge, implementation of a highly complex phytoplankton growth model at an ecosystem scale, coupled to a hydrodynamic model and other biogeochemical compartments; 2) establishing the capacity to reproduce the biogeochemistry of the German Bight both at coastal and off-shore regions with a single parameterization and model setup.

For a 11 year hindcast simulation of the period 2000-2010, we show that the model can adequately capture the spatio-temporal variability of the physical and biogeochemical features of the SNS based on comparisons against various data sources. Importantly, the model can reproduce the steep chlorophyll and nutrient gradients prevalently observed across the Waddensea-German Bight continuum. We show that the chlorophyll gradients are linked with nutrient, hence, productivity gradients, but also further amplified by the high chlorophyll to carbon ratios at the shallower regions owed to the high turbidity.

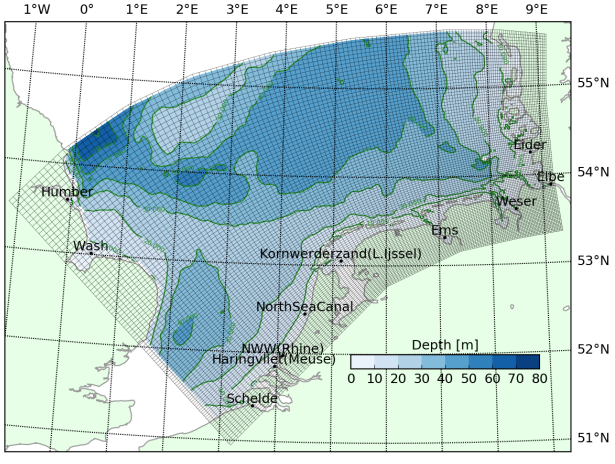

Figure 1. Bathymetry of the model domain and the location of rivers considered in this study. Gray lines display the model grid.

2 Methods

2.1 Data

Data from monitoring stations all reflect surface measurements. Extensive analyses of the data from Helgoland Roads have been provided by Wiltshire et al. (2008) and from Sylt by Loebl et al. (2007). Temperature, salinity, dissolved inorganic nitrogen

Biogeosciences Discuss., doi:10.5194/bg-2017-104, 2017
Manuscript under review for journal Biogeosciences
Discussion started: 30 March 2017

and phosphorus data obtained from the International Council for the Exploration of the Sea (ICES, www.ices.dk) were used for the validation of the physical and biogeochemical model, by means of point-wise comparisons within the surface and bottom layers, i.e., upper and lower 5 meters.

Vertically resolved Scanfish data and continuous Ferrybox measurements were all gathered within the Coastal Observing System for Northern and Arctic Seas (COSYNA, Baschek et al., 2016, and references therein). Satellite data employed here are provided by the European Space Agency (ESA), Ocean Color- Climate Change Initiative version 2.0, where the NASA OC4.V6 algorithm had been applied to the MERIS, MODIS and SeaWiFS products for the estimation of chlorophyll concentrations (Grant et al., 2015).

2.2 Model

Major processes taken into account by the model are the lower trophic food web dynamics, phytoplankton ecophysiology and basic biogeochemical transformations in water, and the transformation of N- and P- species in benthos (Fig.2 and Section 2.2.1). Physical processes are resolved by the coupled 3-D hydrodynamical model, GETM (Section 2.2.2). Turbidity caused by suspended particulate matter (SPM), nutrient loading by rivers and atmospheric nitrogen deposition were considered as model forcing (Section 2.2.3). The model grid and riverine fluxes considered in this study are shown in Fig.1.

2.2.1 Biogeochemical model

The pelagic module, the Model for Adaptive Ecosystems in Coastal Seas (MAECS), is a lower trophic level model that resolves cycling of carbon, nitrogen (N) and phosphorus (P), and importantly, acclimation processes of phytoplankton, a detailed description of which is provided by Wirtz and Kerimoglu (2016) and in the supplementary material (A). The acclimation module features a whole set of physiological traits (x), which control accessory and assimilation of multiple resources in autotrophs. These comprise, affinity for DIN and DIP, protein pools invested to nutrient uptake and light harvesting, and specific P- and N-uptake activities. Their instantaneous or transitory acclimation follows an extended optimality principle,

$$\frac{\mathrm{d}}{\mathrm{d}t}x = \delta_x \cdot \left[\frac{\partial V_\mathrm{C}}{\partial x} + \sum_i \frac{\partial V_\mathrm{C}}{\partial q_i}\frac{\partial q_i}{\partial x}\right] \tag{1}$$

where δ_x corresponds to a flexibility constant, and the two terms in brackets describe the direct effects of trait changes on the specific phytoplankton growth rate V_C (in units of cellular C) and the indirect effects through changes in the Chl:C:N:P stoichiometry, expressed by the quotas q, respectively (Wirtz and Kerimoglu, 2016). As a result of trait variations formulated in Eq.1, Chl:C:N:P stoichiometry is continuously varied depending on ambient light and nutrient conditions and on the metabolic demands of autotrophic cells.

Other components of the pelagic module are similar to standard descriptions in state-of-the-art ecosystem models. Phytoplankton take up nutrients in the form of dissolved inorganic material (DIM). Losses of phytoplankton (B) and zooplankton (Z) due to mortality are added to the particulate organic matter (POM) pool, which degrades into dissolved organic material (DOM), before becoming again DIM and closing the cycle.

Biogeosciences Discuss., doi:10.5194/bg-2017-104, 2017
Manuscript under review for journal Biogeosciences
Discussion started: 30 March 2017

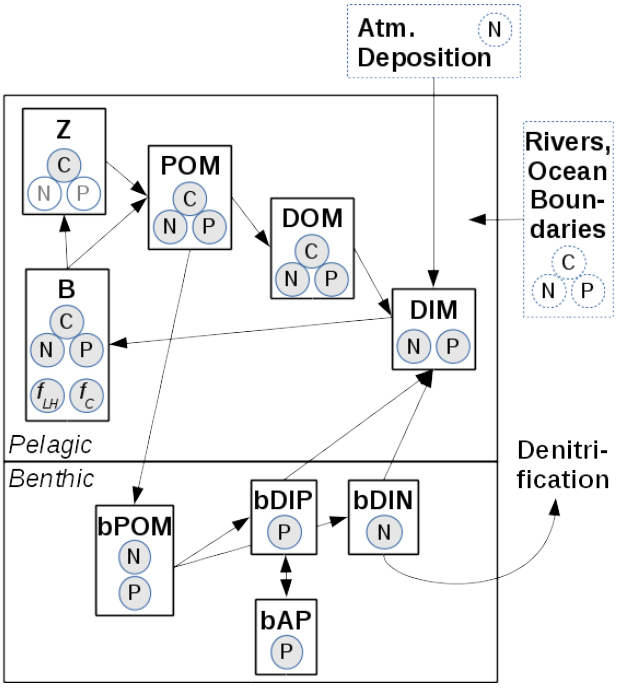

Figure 2. Structure of the biogeochemical model. Model components (rectangles) comprise; B: phytoplankton, Z: zooplankton, POM and DOM: particulate and dissolved organic matter, DIM(N,P): dissolved inorganic matter (nitrogen,phosphorus), Fe-P: P adsorbed in iron-phosphorus complexes (See Section 2.2.1 and supplementary material A for further details). C, N, P in small circles refer to carbon, nitrogen and phosphorus bound to each component, respectively, whereas f_{LH} and f_C are the allocation coefficients for light harvesting and carboxylation (Section 2.2.1). Boxes in dashed lines indicate model forcing.

The benthic module describes only the dynamics of macronutrients N and P. Degradation of OM to DIM is described as a one step, first order reaction. Denitrification is described as a proportion of POM degradation, limited by DIN and dissolved oxygen (DO) availability in benthos. As DO is not directly modeled, it is estimated from temperature in order to mimic the seasonality of the hypoxia-driven denitrification. The model accounts for the sorption-desorption dynamics of phosphorus as an instantaneous process also as a function of temperature based on the correlation observed in the field (Jensen et al., 1995). Further details are provided in Appendix A.

2.2.2 Hydrodynamic model and model coupling

The General Estuarine Transport Model (GETM) was used to calculate various hydrodynamic processes, as well as the transport of the biogeochemical variables. A detailed description of GETM is provided by Burchard and Bolding (2002); Stips et al. (2004). GETM utilizes the turbulence library of the General Ocean Turbulence Model (GOTM) to resolve vertical mixing of density and momentum profiles with a k-ε two equation model (Burchard et al., 2006). GETM was run in baroclinic mode, resolving the 3-D dynamics of temperature, salinity and currents and 2-D dynamics of sea surface elevation and flooding-

Biogeosciences Discuss., doi:10.5194/bg-2017-104, 2017
Manuscript under review for journal Biogeosciences
Discussion started: 30 March 2017

drying of cells at the Wadden Sea. We used 20 terrain-following layers and a curvilinear grid of 144x98 horizontal cells with a horizontal resolution of approximately 1.5 km at the south-east corner and 4.5 km at the north-west corner (Fig. 1). The curvilinear grid focuses on the German Bight, and roughly follows the coastline (Fig. 1) for an optimal representation of along- and across- shore processes. Similar gridding strategies were applied successfully in other coastal setups with the GETM model (Hofmeister et al., 2013; Hetzel et al., 2015). We employed integration time steps of 5 and 360 seconds for the 2-D and 3-D processes, respectively.

Integration of model forcing was realized through the Modular System for Shelves and Coasts (MOSSCO, http://www.mossco.de), which among others, provides standardized data representations. Meteorological forcing originated from an hourly-resolution hindcast by COSMO-CLM (Geyer, 2014). Boundary conditions for surface elevations and currents are extracted from an hourly resolution hindcast by TRIM-NP (Weisse et al., 2015). For temperature and salinity, daily climatologies from HAMSOM (Meyer et al., 2011) are used, all of which are available through coastDat http://www.coastdat.de.

Two-way coupling of the biological model with GETM was achieved via the Framework for Aquatic Biogeochemical Models (FABM, Bruggeman and Bolding, 2014) as one of the coupling standards adopted in MOSSCO. The pelagic module is defined in the 3-D grid of the hydrodynamic model, whereas the benthic module is defined in 0-D boxes for each water column across the lateral grid of the model domain (Fig. 1). Each benthic box interacts with the bottom-most pelagic box of the corresponding water column in terms of a uni-directional flux of POM from the pelagic to the benthic states, and a bi-directional flux of DIM depending on the concentration gradients.

For the integration of the source terms, a fourth order explicit Runge-Kutta scheme was used with an integration time step of 360 seconds, as for the 3-D fields in GETM. Exchange between pelagic and benthic variables was integrated with a first order explicit scheme at a time step identical to that of the biological model.

2.2.3 Model forcing and boundary conditions

Light extinction is described according to:

$$I(z) = I_0 a e^{-\frac{z}{\eta_1}} + I_0(1-a)e^{-\frac{z}{\eta_2} - \int_z^0 \sum_i k_{c,i} c_i(z')dz'} \quad (2)$$

where, I_0 is the photosynthetically available radiation at the water surface, and the first and second terms describe the attenuation at the red and blue-green portions of the spectrum. We assume that the partitioning of the two (a) and the attenuation length scale of the red light (η_1) are constant over space and time as in Burchard et al. (2006), and that the attenuation of blue-green light is due to SPM (as described by η_2) and organic matter (sum term). We chose $a = 0.58$ and $\eta_1 = 0.35$, which correspond to Jerlov class-I type water, thus clear water conditions (Paulson and Simpson, 1977), given that the attenuation by SPM and organic matter is explicitly taken into account. For calculating attenuation due to SPM, a daily climatology of SPM concentrations defined over the model domain was utilized, like in ECOHAM (Große et al., 2016). The SPM field was constructed by multiple linear regression of salinity, tidal current speed and depth for each Julian day (Heath et al., 2002). Then, η_2, or the inverse of SPM caused attenuation coefficient was calculated according to:

$$1/\eta_2 = k_{SPM} = K_w + \epsilon_{SPM} * SPM \quad (3)$$

Biogeosciences Discuss., doi:10.5194/bg-2017-104, 2017
Manuscript under review for journal Biogeosciences
Discussion started: 30 March 2017

where, the attenuation for background turbidity, $K_w = 0.16$ m^{-1} and specific attenuation coefficient for SPM, $\epsilon_{SPM} = 0.02$ m^2 g^{-1} according to Tian et al. (2009). For calculating the attenuation due to organic matter in Eq.(2), phytoplankton, POC and DOC were considered (Table A3).

Freshwater and nutrient influxes were resolved for eleven major rivers along the German, Dutch, Belgian and British coasts (Fig.1). For eight of these rivers, Radach and Pätsch (2007) and Pätsch and Lenhart (2011) present a detailed quantitative analysis of nutrient fluxes. Besides the fluxes in inorganic form based on direct measurements, fluxes in organic form have been accounted for, first by calculating the total organic material concentration by subtracting dissolved nutrient concentrations from total nitrogen and total phosphorus, then by assuming 30 % of the organic material to be in particulate form (i.e., POM; Amann et al., 2012). Further, 20 % of POM is assumed to describe phytoplankton biomass (Brockmann, 1994), C:N:P ratio of which was assumed to be in Redfield proportions. Finally, no estuarine retention/enrichment was assumed, following Dähnke et al. (2008). All river data except for the river Eider were available in daily resolution, however with gaps. Short gaps (<28 days) were filled by linear interpolation. Loadings from the river Eider were calculated first by merging the data measured at the stations on two upstream branches, Eider and Treene, then by filling the short gaps (<28 days) by linear interpolation, replacing the larger gaps with daily climatology, and extending for 2000-2003 by using the climatology as well. To describe DIN deposition at the water surface, sum of annual average atmospheric deposition rates of NO_x and NH_3 provided by EMEP (European Monitoring and Evaluation Programme, http://www.emep.int) were used. At the open boundaries in the north and west of the model domain (Figure 1), all state variables belonging to the phytoplankton and zooplankton compartments are assumed to be at zero-gradient. For DIM, DOM and POM, monthly values of ECOHAM (Große et al., 2016), interpolated to 5m depth intervals are used as clamped boundary conditions.

2.3 Quantification of Model Performance

For the comparisons with the station data for DIN, DIP and Chl concentrations, Pearson correlation coefficients were calculated for all temporal matches. For the evaluation of model performance against the ICES data for temperature, salinity, DIN and DIP, correlation scores and model standard deviations normalized to measured standard deviations are displayed as Taylor diagrams, where the correlation score and the normalized standard deviation correspond to the angle and distance to the center (Jolliff et al., 2009). For this purpose, temporal matching was identified at daily resolution, vertical matching were obtained by comparing the measurements within the upper 5 meters from the sea surface and within the 5 meters above the sea floor with the model estimates at the top-most and bottom-most layers, and finally lateral matching by calculating the average of the values from four cells surrounding the measurement location, inversely weighted with respect to the Cartesian distance. Finally, comparison of the spatial structure of the model estimates to that of the satellite (ESA-CCI) data was achieved also through Taylor Diagrams. For this purpose, temporal matching was obtained by averaging the data from both sources for the period 2008-2010 for particular seasons of the year, and lateral matching by performing a 2-dimensional linear interpolation of the satellite data to the model grid. For the comparisons against the ICES and ESA-CCI data, only the middle-99 percentile of model and measurements were considered (i.e., leaving out the first and last 0.05th percentiles).

Biogeosciences Discuss., doi:10.5194/bg-2017-104, 2017
Manuscript under review for journal Biogeosciences
Discussion started: 30 March 2017

3 Results and Discussion

3.1 Evaluation of Model Performance by in-situ Data

A comparison of simulated salinities with the FerryBox measurements along the cruise between Cuxhaven (at the mouth of river Elbe) and Immingham (at the mouth of river Humber) (Petersen, 2014), demonstrates that the model captures the general salinity patterns (Fig.3). However, the freshwater plume in the German Bight as simulated by GETM seems to extend further from the coast than observed, which suggests moderate over-estimation of horizontal mixing by the model.

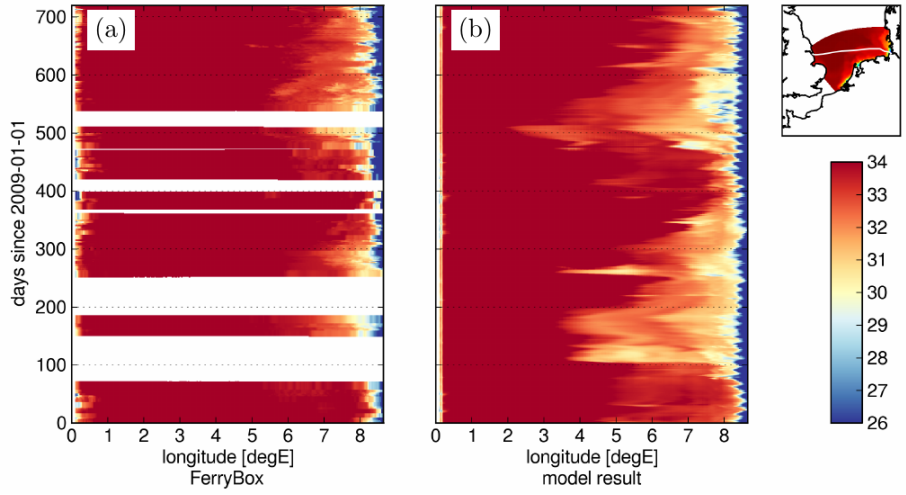

Figure 3. Salinity [PSU] measured by ferry-box (a) and estimated by the model (b) along the route shown in the inset

Comparison of simulated surface and bottom temperatures with those extracted from the ICES data set for the period 2006-2010 are provided in Fig. 4. High correlation scores ($\geq$0.85 for surface and $>$0.9 for bottom layers) attained for water temperature and salinity suggest that the model can generally reproduce the seasonal warming, spread of freshwater discharges and stratification dynamics driven by temperature and salinity gradients. However, surface temperatures are in part underestimated and bottom temperatures are overestimated, which indicates that not all stratification events were captured. Most of the mismatch in salinity occur at the lower range, in the form of a systematic underestimation in both surface and bottom layers, resulting in a higher standard deviation of the model estimates relative to the measurements. Further analysis (not shown) revealed that this problem was most pronounced in 2010, which was a relatively wet year, indicating again that the model overestimates the transport of freshwater from rivers especially during high-discharge events, which points to the deficiency of the grid resolution to capture such events realistically.

Comparisons of model-estimated surface chlorophyll, DIN and DIP with the measurements in 19 stations scattered across the southern North Sea (Fig. 5-Fig.7) yields following: *i*) there are no obvious decadal trends neither in observations, nor in simulated values. *ii*) Average and peak nutrient and chlorophyll concentrations are in general well reproduced. In some coastal stations, like Sylt, chlorophyll concentrations seem to be overestimated although the nutrient concentrations are rather

Biogeosciences Discuss., doi:10.5194/bg-2017-104, 2017
Manuscript under review for journal Biogeosciences
Discussion started: 30 March 2017

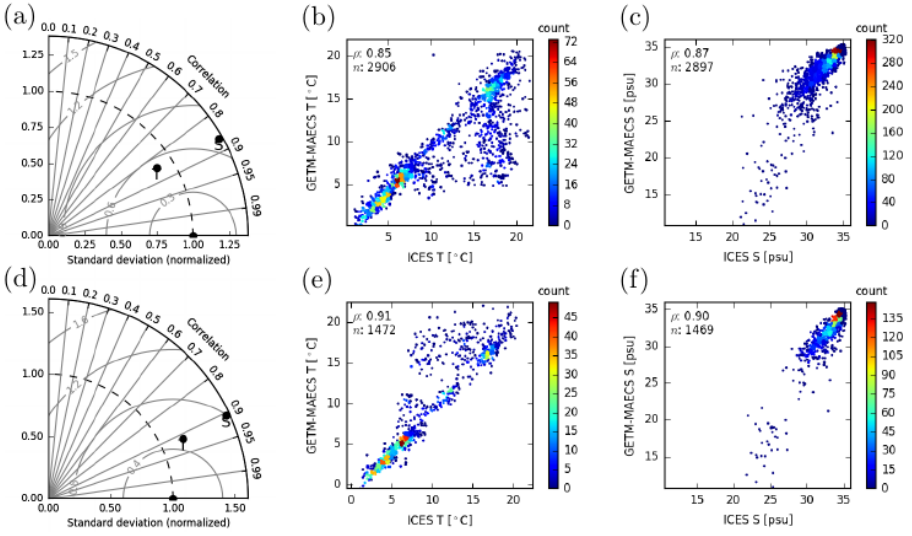

Figure 4. Comparison of modeled and measured (ICES) temperature (abbreviated T in panels a,d,b,e) and salinity (abbreviated S in a,d,c,f) at the surface (a-c) and bottom (d-f) layers for the period 2006-2010. 2-D histograms show the number of occurrence of simulation-measurement pairs.

realistically represented. In a few other stations like Norderelbe and Noordwijk, nutrient concentrations are not very realistic: given the proximity of these stations to major rivers Elbe, North Sea Canal and Rhine (Fig.1), these mismatches are likely to be related with our assumption that the non-dissolved fractions of the total nitrogen and total phosphorus to be all in labile form (Sect. 2.2.3). *iii*) Timing of spring blooms, nutrient draw-down and regeneration are mostly well reproduced, as also reflected by high correlation coefficients in general. Earlier replenishment of phosphorus relative to nitrogen is often reproduced, although with delays in some coastal stations like Norderney, which probably reflects the oversimplification of the benthic processes with respect to the description of oxygen-driven iron-phosphorus complexation kinetics (Sect. A), which has been suggested to be the main driver for the phenomena in the coastal areas (Jensen et al., 1995; van Beusekom et al., 1999; Grunwald et al., 2010). Finally, measurements from S. Amrum suggest that the classical summer-low, winter-high phosphorus pattern, as also predicted by our model in general, is entirely reversed, calling for a more detailed investigation.

There are a number of caveats when using coastal time-series data for model validation, which start from the sampling problem: short term fluctuations common for near-shore waters can only be tentatively represented by measurement frequencies of several weeks or months. For the special case of Sylt, for example, data reflect the average monthly concentrations, which naturally smooths out the short-lived blooms. However, we acknowledge the potentially inadequate description of certain processes that might have led to the overestimation of chlorophyll concentrations at Sylt, such as the grazing formulation of zooplankton and the representation of the light climate. In reality, effects of temperature on mesozooplankton occurs through phenological shifts (e.g., Greve et al., 2004) that might have a determining role on the maximum chlorophyll concentrations (van Beusekom et al., 2009), which can probably be only partially reflected by the simple Q10 rule we applied for grazing

Biogeosciences Discuss., doi:10.5194/bg-2017-104, 2017
Manuscript under review for journal Biogeosciences
Discussion started: 30 March 2017

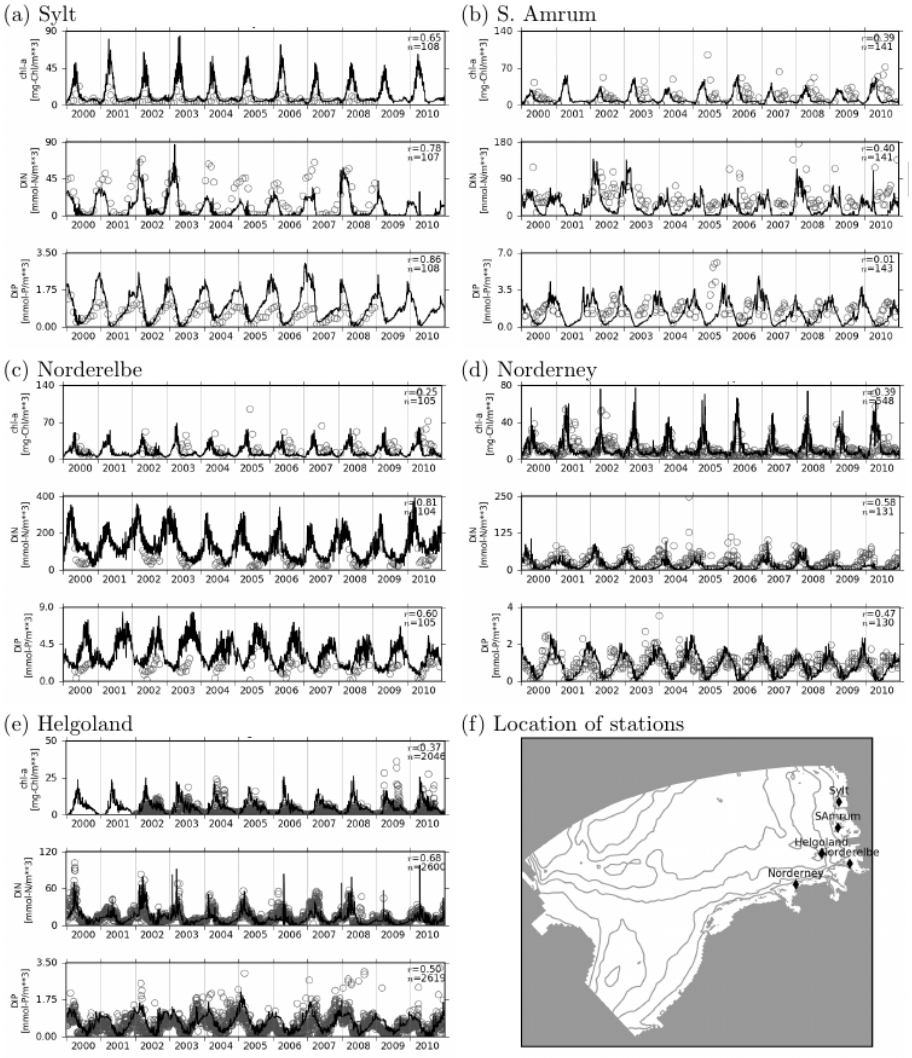

Figure 5. Observations and model estimates of surface chlorophyll, DIN and DIP concentrations at the stations located along the coasts of the German Bight, operated by Alfred Wegener Institute (Helgoland and Sylt), Landesamt für Landwirtschaft, Umwelt und ländliche Räume des Landes Schleswig-Holstein (S. Amrum, Norderelbe) and Niedersächsischer Landesbetrieb für Wasserwirtschaft, Küsten- und Naturschutz (Norderney). Pearson correlation coefficients, and corresponding number of data points are shown at the top-right corner.

rates (Sect. A1). Light climate on the other hand, especially in the shallow regions in the German Bight, is largely influenced by SPM concentrations (Tian et al., 2009), which is here provided to the model as a daily climatological forcing (Sect. 2.2.3), hence, neglecting any potential inter-annual variability.

Taylor diagrams for DIN and DIP at the surface and bottom layers (Fig. 8) indicate a reasonable match to the ICES data for the period 2000-2010. Comparison of surface and bottom data separately prevents the domination of the performance statistics

Biogeosciences Discuss., doi:10.5194/bg-2017-104, 2017
Manuscript under review for journal Biogeosciences
Discussion started: 30 March 2017

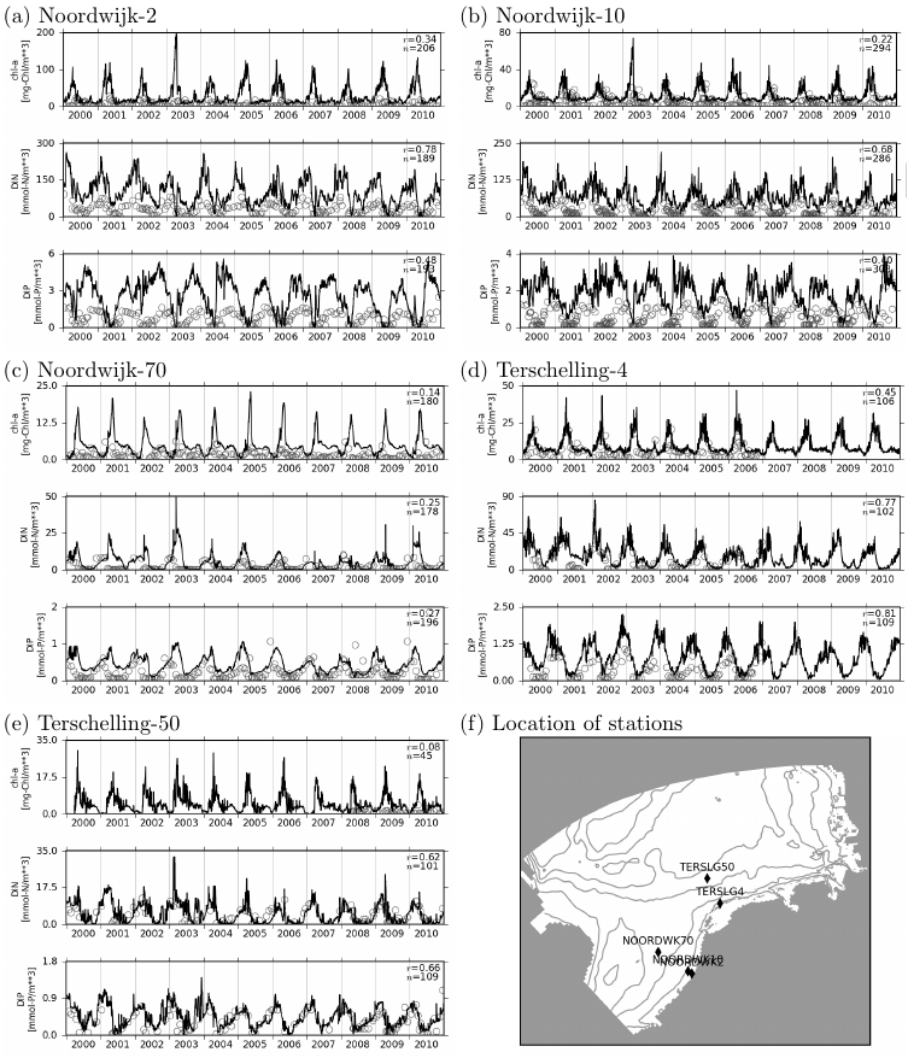

Figure 6. As in Fig. 5, but for the stations located along the coasts of the Netherlands, operated by Rijkswaterstaat.

by strong differences between the surface and bottom layers which are relatively easier to reproduce, as would be captured by the correlation scores. Therefore, the comparison with the ICES data rather reflects the ability of model to capture the lateral and temporal (at seasonal and inter-annual scales) variability of DIN and DIP. Modeled variability matches very well to the observed variability for both DIN and DIP at the surface and DIN at the bottom layer. However, the variability of DIP at the bottom layer is overestimated, which seems to be caused by the occasional overestimation of the values at the higher range (1-2 mmolP/m^3), which, again, might be related with the oversimplified representation of phosphorus dynamics in the sediment. Correlation coefficients obtained for DIN and DIP both at the surface and bottom layers seem to be relatively high, considering the typical skill level of coupled physical-biogeochemical models in estimating nutrient concentrations for the

Biogeosciences Discuss., doi:10.5194/bg-2017-104, 2017
Manuscript under review for journal Biogeosciences
Discussion started: 30 March 2017

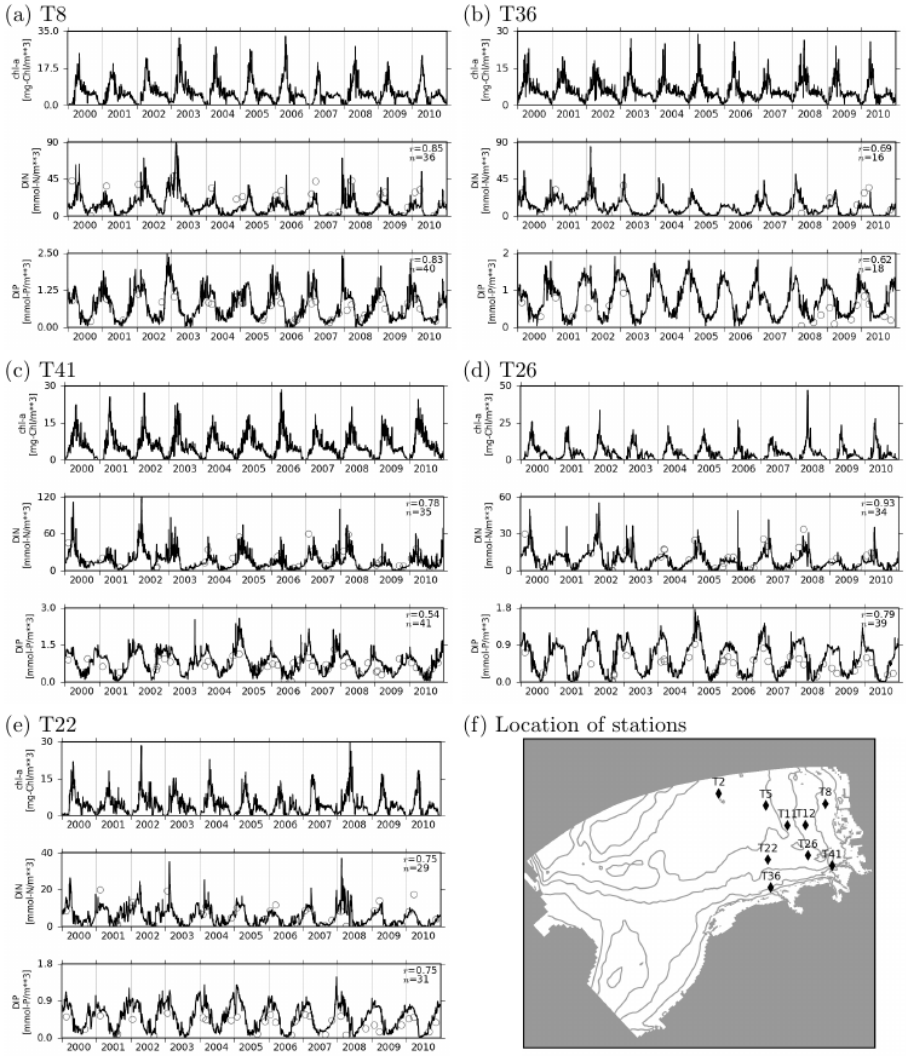

(continued on the next page)

North Sea (e.g., Radach and Moll, 2006; Daewel and Schrum, 2013; de Mora et al., 2013), noting, however that a conclusive model inter-comparison would require standardized benchmarking data set and procedures.

For an assessment of the accuracy of the simulated vertical distributions, water density (expressed as σ_T) and fluorescence captured by a Scanfish cruise (Heincke-331) obtained during 13-19 July 2010 were compared to those estimated by the model (chlorophyll for fluorescence) averaged over the same time period (Fig.9). σ_T transect reflects two major mechanisms: first is the vertical gradients characterized by denser water at the bottom layers, which is mainly driven by thermal stratification as suggested by temperature profiles (not shown). Second is the horizontal gradients characterized by lighter water at the coasts, driven by low salinity due to the freshwater flux from the rivers. The model can accurately reproduce both vertical

Biogeosciences Discuss., doi:10.5194/bg-2017-104, 2017
Manuscript under review for journal Biogeosciences
Discussion started: 30 March 2017

(continues from the previous page)

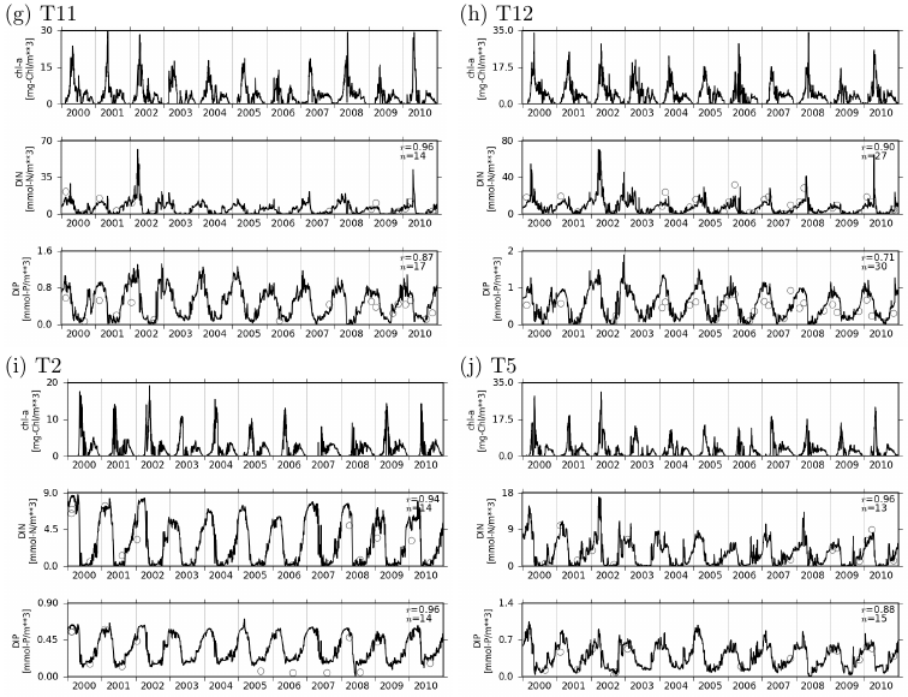

Figure 7. As in Fig. 5, but for the off-shore monitoring stations operated by Bundesamt für Seeschifffahrt und Hydrographie.

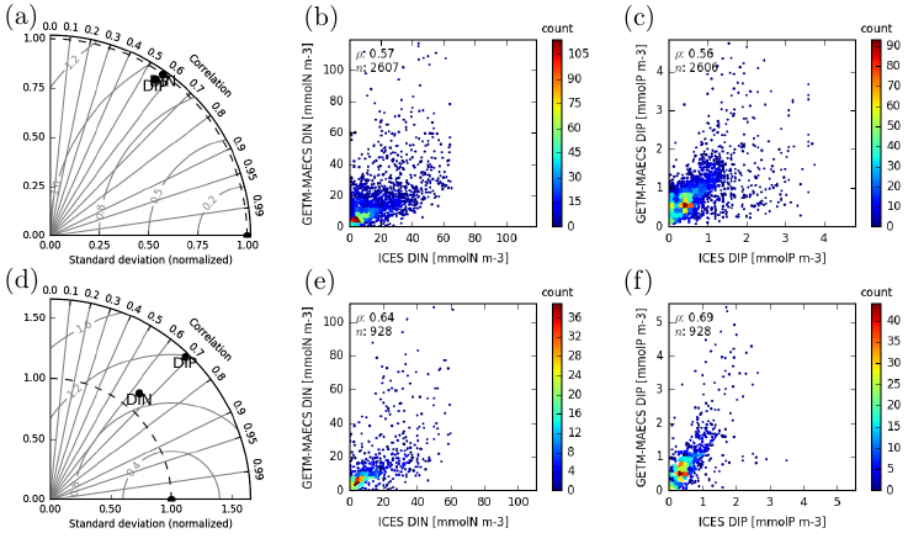

Figure 8. Comparison of simulated and measured (ICES) DIN (a,d,b,e) and DIP (a,d,c,f) at the surface (a-c) and bottom (d-f) layers for the period 2000-2010. 2-D histograms show the number of occurrence of simulation-measurement pairs.

Biogeosciences Discuss., doi:10.5194/bg-2017-104, 2017
Manuscript under review for journal Biogeosciences
Discussion started: 30 March 2017

and horizontal density gradients, except small discrepancies such as slightly overestimated densities at the bottom layers and steepness of lateral gradients at around the coastal section.

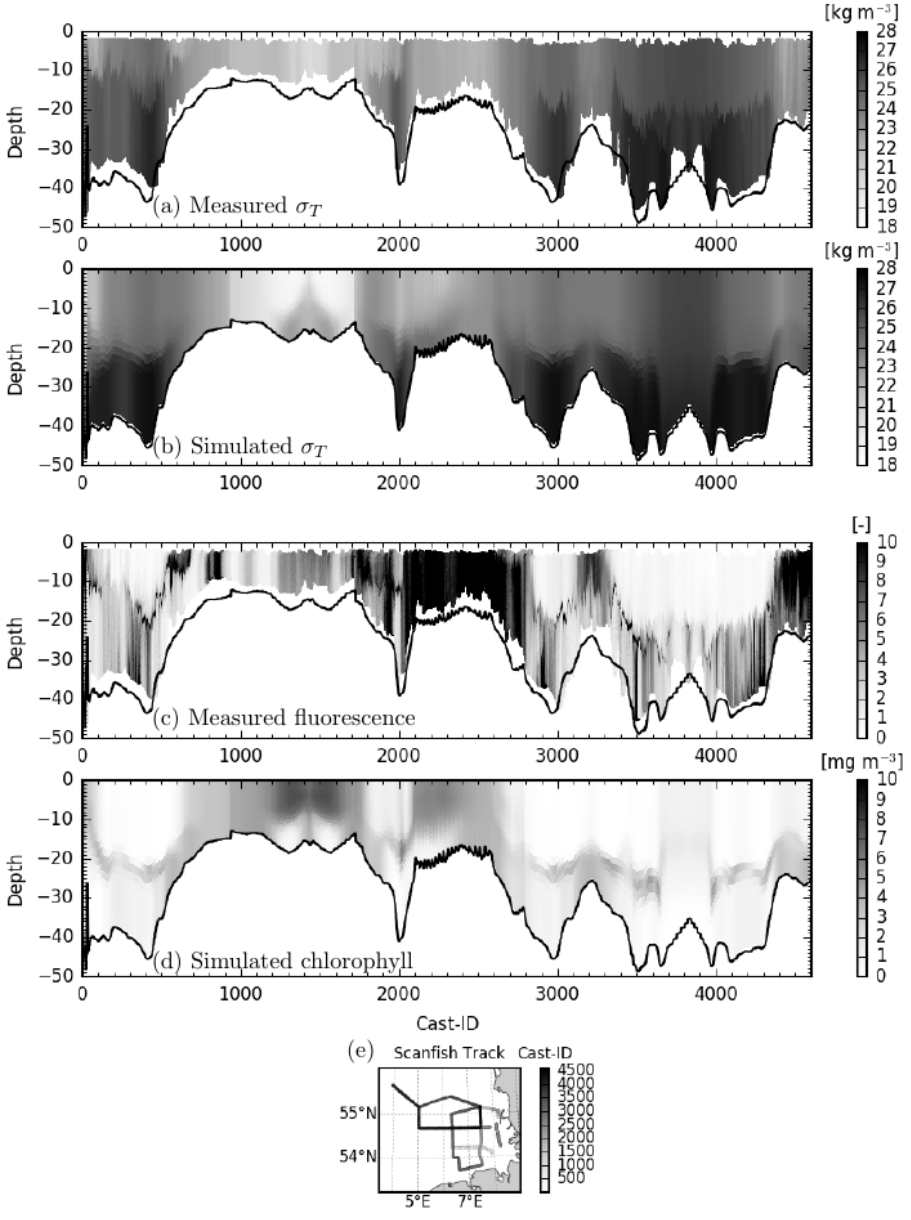

Figure 9. σ_T (a) and fluorescence (c) measured by Scanfish recorded during 13-19 July 2010 compared to σ_T (b) and chlorophyll concentration (d) estimated by the model averaged throughout the same period. Black line indicates the sea floor. Cruise track shown in (e).

Fluorescence measurements along the Scanfish track in July 2010 indicate frequent occurrences of deep-chlorophyll maxima (Fig.9), in accordance with previous observations (Weston et al., 2005; Fernand et al., 2013). These deep-chlorophyll maxima

are in some cases in the form of higher concentrations below the pycnocline but in some others, appear as thin layers around the pycnocline. While deep chlorophyll maxima are visible in stratified waters that occur in deeper regions, well-mixed shallower regions mostly show vertically homogeneously distributed high chlorophyll concentrations. The MAECS simulation agrees qualitatively very well with these patterns and captures the spatial variability of the observed vertical chlorophyll distribution (Fig.9). Former 3-D modeling studies, such as that of van Leeuwen et al. (2013), apart from capturing the presence of a deep chlorophyll maximum, were not able to reproduce the rich variability revealed by the observations. Our model-based analysis indicates that the formation and maintenance of such structures are critically dependent on the parametrization of the underwater light climate and sinking rate of phytoplankton. Sinking speed of algae in the MAECS is inversely related to the nutrient quota of the cells, which mimics the internal buoyancy regulation ability of algae depending on internal nutrient reserves (see section A1) but also indirectly emulates chemotactic migration as typical for dinoflagellates (Durham and Stocker, 2012). The critical dependence of the formation and maintenance of vertical chlorophyll structures on the functional representation of sinking underlines the relevance of an accurate description of the intracellular regulation of nutrient storages and pigmentory material.

3.2 Coastal Gradients

Temperature stratification is one of the key drivers of biogeochemical processes through its determining role on the resource environment, i.e., light and nutrient availability experienced by the primary producers. The comparison against Scanfish transect (Fig.9) indicated that our model can capture density stratification quite accurately. Using the temperature difference between surface and bottom layers as an indicator of temperature stratification (Schrum et al., 2003; Holt and Umlauf, 2008; van Leeuwen et al., 2015), and using monthly averages across all simulated years (2000-2010), we illustrate the areal extent and seasonality of stratification within the SNS in Fig.10. This analysis suggests that a large portion of the model domain deeper than $\sim$30 m becomes stratified from April to September, with maximum intensity and areal coverage in July. The areal extent and seasonality of stratification is in agreement with those reported by earlier studies (Schrum et al., 2003; van Leeuwen et al., 2015).

Average winter concentrations of surface DIN and DIP for the entire simulation period display steep gradients along the coasts of the German Bight (Fig. 11), in line with observations (e.g., Brockmann et al., 1999). Given the riverine nutrient fluxes and uninterrupted nutrient supply from the bottom layers owed to the lack of stratification (Fig. 10), it is not surprising that the surface nutrient concentrations are higher at the coasts, but the persistence of the phenomenon in the Wadden Sea regions that are not in close proximity to the riverine fluxes and the steepness of these gradients are not intuitively predictable. Steep cross-shore nutrient gradients were partially explained by an interplay between density gradients and tidal mixing: during tidal flooding, high-salinity, therefore denser off-shore water sinks below the low-salinity, therefore lighter coastal water, thereby pushing the nutrient-rich bottom waters towards the coast (Ebenhöh, 2004; Burchard et al., 2008; Flöser et al., 2011; Hofmeister et al., 2016). The relevant physical processes, i.e. tidal assymmetries in currents and mixing under coastal density gradients, and the accumulation of nutrients at the bottom layers in off-shore waters are represented in the current model framework, so that this residual density-driven circulation mechanism is likely to be responsible for the emergence of steep nutrient gradients

Biogeosciences Discuss., doi:10.5194/bg-2017-104, 2017
Manuscript under review for journal Biogeosciences
Discussion started: 30 March 2017

Biogeosciences Discussions Open Access EGU

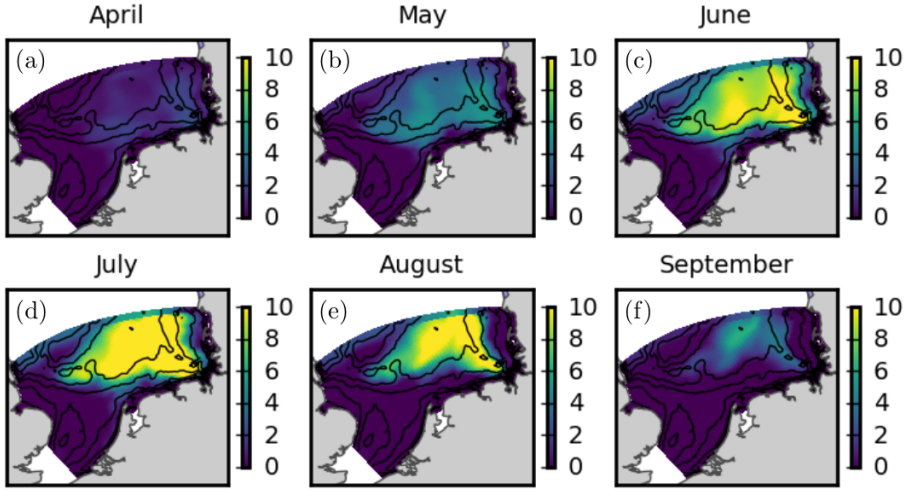

Figure 10. Average temperature difference [K] between the surface and bottom layers, averaged throughout 2000-2010 for each month

shown in Fig.11. Productivity-enhanced aggregation of particulate organic matter with suspended sediments, and hence, higher sedimentation velocities within the coastal transition zone has recently been proposed to be another contributing factor for the maintenance of the coastal nutrient gradients (Maerz et al., 2016). This process has not been accounted for by our model, and representation of such a mechanism would necessitate explicit descriptions of mineral-POM interactions and variable sinking rate as a function of particle composition, structure and size (Maerz et al., 2011). An exhaustive elaboration of the mechanisms for the maintenance of such gradients, their regional variability and steepness would be out of the scope of the current work, but constitutes a potential research goal for the future.

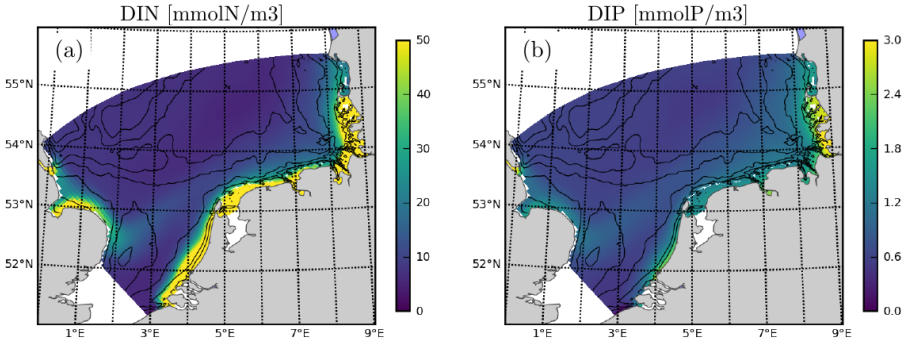

Figure 11. Winter (January-February) DIN (a) and DIP (b) concentrations averaged over the period 2000-2010

Interestingly, within the eastern portion of the model domain, the range of N:P ratios in DIM gradually decrease with bottom depth according to both the model estimates and ICES measurements (Fig. 12). Higher N:P ratios, which are mostly found at the shallower sites, i.e., closer to the coast should be associated with the high N:P ratios at the continental rivers (Radach

Biogeosciences Discuss., doi:10.5194/bg-2017-104, 2017
Manuscript under review for journal Biogeosciences
Discussion started: 30 March 2017

and Pätsch, 2007). Lower N:P ratios on the other hand, which, in a majority of cases, are recorded during the growth season, presumably results from a complex interplay between phytoplankton growth, sedimentation, denitrification and phosphorus absorption/desorption dynamics. The extent to which individual processes drive the regulation of water stoichiometry, and the implications of these changing external N:P ratios, e.g., on the competition between different phytoplankton species, remain to be an open questions.

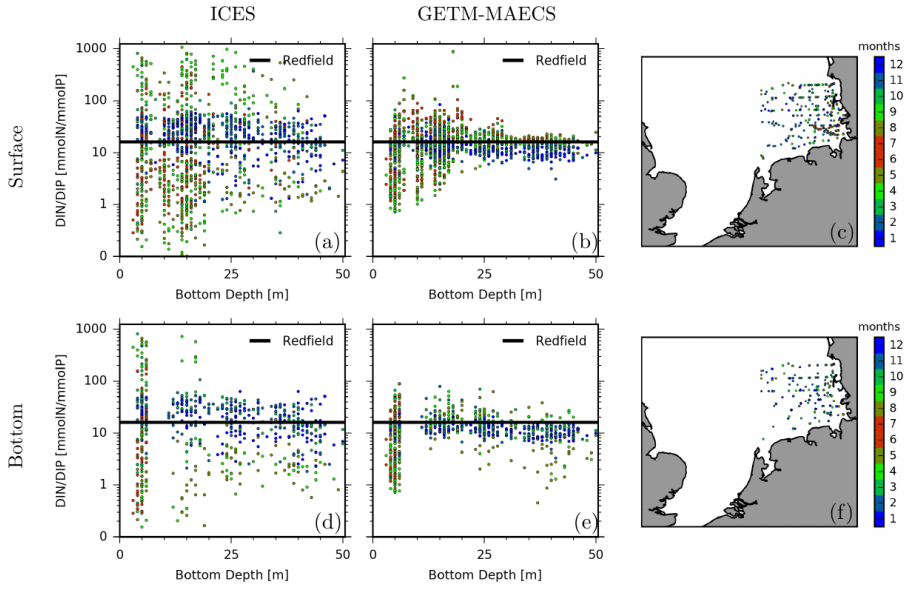

Figure 12. DIN:DIP ratio in water binned over 1 m bottom depth intervals according to ICES data (a,d) and matching MAECS results (b,e) at the surface (a-c) and bottom (d-f) layers, within the eastern portion of the model domain ($> 5°$E, exact locations shown in c and f)

Both the satellite (ESA-CCI) images and our model estimates, averaged over the years 2008-2010 for the two halves of the growing season, suggest much higher concentrations within a thin coastal stripe relative to the off-shore concentrations. The large scale agreement in coastal gradients result in high correlation coefficients, especially during summer (Fig.13). For the first half of the growing season, the higher range of the modelled chlorophyll values exceed those of the ESA-CCI (Fig.13), which seems to be caused by underestimation by the satellite product, suggested by the fact that *in-situ* concentrations frequently reach well over 50 mg/m^3 at the coastal stations in the German Bight (Fig.5). These lateral gradients in chlorophyll concentrations overlap with the nutrient (Fig.11), hence, productivity gradients (not shown).

According to our simulation results of the year 2010, average Chl:C ratio displays considerable spatio-temporal variability, even when the seasonal averages are considered, i.e., omitting short-term variability (Fig.14). Chl:C ratio is in general higher at the coasts than at off-shore. This pattern has been previously identified based on monitoring data by Alvarez-Fernandez and Riegman (2014), and reflects the photoacclimative response to stronger light limitation at the coasts, manifested by both higher organic matter (not shown, but see Fig.13 for chlorophyll concentrations) and SPM concentrations. Higher Chl:C ratios during the non-growing (months 10-12 and 1-3) season similarly reflects light limitation due to low amounts of incoming short

Biogeosciences Discuss., doi:10.5194/bg-2017-104, 2017
Manuscript under review for journal Biogeosciences
Discussion started: 30 March 2017

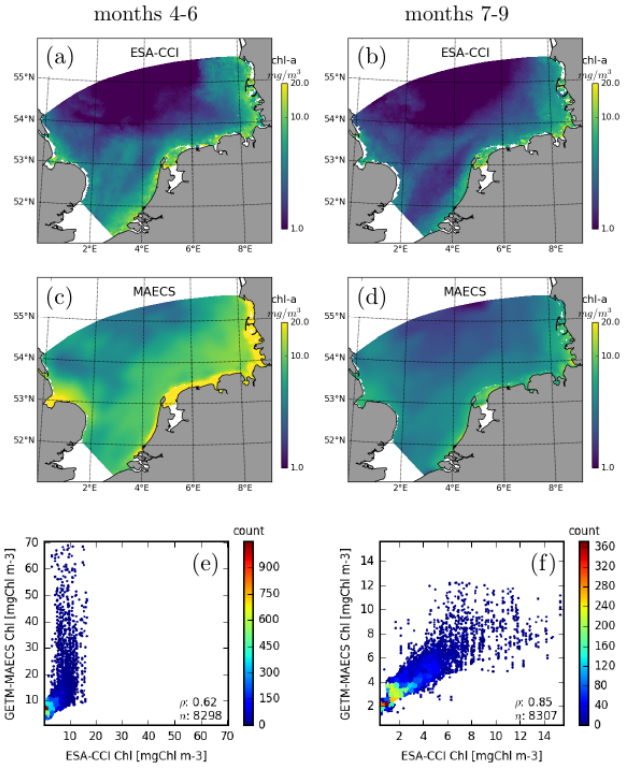

Figure 13. Comparison of satellite (ESA-CCI, a,b) and MAECS (c,d) estimates of surface chlorophyll concentrations averaged over 2008-2010 and for different seasonal intervals of the year. 2-D histograms (e,f) show the number of occurrence of simulation-satellite data pairs.

wave radiation at the water surface and increased turbidity due to stronger vertical mixing near the coast. A similar seasonal amplitude in CHL:C has been found by Llewellyn et al. (2005) for the English Channel. Slightly higher Chl:C ratios during the first half of the growing season compared to the second half are likely due to lower nutrient concentrations during the second half, which results in larger investments in nutrient harvesting in the expense of light-harvesting machinery (see, e.g., Geider et al., 1997; Pahlow, 2005; Wirtz and Kerimoglu, 2016). The modeled spatio-temporal differences in Chl:C ratios reach to about three fold between different seasons of the year and between off-shore and coastal areas. The latter indicates that the differential acclimative state of phytoplankton cells amplify the steepness of the chlorophyll gradients across the coastal transition shown in Fig. 13, which, as mentioned above, seem to be driven mainly by nutrient gradients. This is significant, and calls for further attention, especially given that many modelling schemes applied at ecosystem-scales do not consider photoacclimation processes. As Behrenfeld et al. (2015) recently pointed out from a global perspective, satellite-based primary productivity estimates can be misleading when they do not take the variability in Chl:C into account. Our results suggest that this caveat holds for the coastal ocean, characterized by relatively high production rates.

Biogeosciences Discuss., doi:10.5194/bg-2017-104, 2017
Manuscript under review for journal Biogeosciences
Discussion started: 30 March 2017

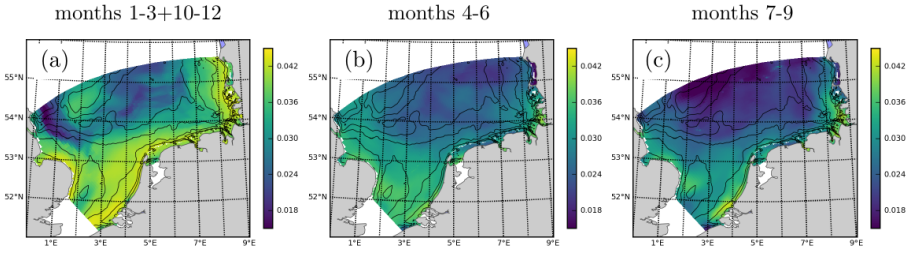

Figure 14. Chlorophyll:C ratio in phytoplankton, averaged over non-growing (a) and two halves of the growing season (b,c) of 2010.

4 Conclusions

In this study, we described the implementation of a coupled physical-biogeochemical model to the Southern North Sea (SNS) and analyzed the model results in comparison to a large collection of *in-situ* and remote sensing data. The model system accounts for key coastal processes, such as the forcing by local atmospheric conditions, riverine loadings of inorganic and organic material, atmospheric nitrogen deposition, spatio-temporal variations in the underwater light climate, major benthic processes and nutrient concentrations at open boundaries, and importantly, it hosts a novel model of phytoplankton growth, which replaces otherwise heuristic formulations of photosynthesis and nutrient uptake with mechanistically sound ones (Wirtz and Kerimoglu, 2016). Based on comparisons with a number of data sources, we conclude that the model system can produce a realistic decadal hindcast of the SNS for the period 2000-2010, in terms of both the temporal and spatial distribution of key ecosystem variables, as well as a large area of validity, i.e., both in coastal and off-shore regions of the German Bight.

We emphasize that even the phytoplankton concentrations are generally well captured by our model, considering the systematic difficulties in reproducing chlorophyll concentrations by ecosystem models in general (see, e.g., Radach and Moll, 2006). This is noteworthy, given that phytoplankton is represented by a single species in our model, whereas in reality the phytoplankton composition displays systematic shifts throughout the season: the early spring composition is usually dominated by diatoms while other species or groups usually become more abundant later in the year, such as *Phaeocystis* at coastal regions (eg., van Beusekom et al., 2009) and dinoflagellates off-shore (Freund et al., 2012; Wollschläger et al., 2015). We argue that the ability of our model to capture both the spring and summer is, to a great extent, owed to the fact that photoacclimation and optimality in nutrient uptake processes were accounted for. In reality, environmental change, e.g., improvement of light conditions and depletion of nutrient concentrations from spring to summer, promotes the species which have more suitable traits, e.g., regarding light and nutrient utilization. In 3-D model applications so far, photoacclimation of phytoplankton has been either ignored altogether, or it was accounted for in a heuristic sense, where the change in Chl:C ratio is described based on an empirical relationships (Blackford et al., 2004; Fennel et al., 2006). In our model, adaptation of the phytoplankton community to the light and nutrient environment is represented by dynamically changing and instantaneously optimized trait values as described extensively by (Wirtz and Kerimoglu, 2016). Other potentially relevant selection factors, such as the changes in the community structure of heterotrophic grazers (Alvarez-Fernandez et al., 2012; Löder et al., 2012; Beaugrand et al., 2014) or limitation of diatoms by silicate (Loebl et al., 2009) are omitted in this study, and remain to be future research goals, along with

Biogeosciences Discuss., doi:10.5194/bg-2017-104, 2017
Manuscript under review for journal Biogeosciences
Discussion started: 30 March 2017

other model refinements like improving the descriptions of the benthic processes and benthic-pelagic exchange, light climate as a function of SPM dynamics and composition of riverine nutrient fluxes.

Our findings suggest that the steep chlorophyll gradients across the coastal transition zone is mainly driven by the nutrient gradients, but amplified by the higher Chl:C ratios at the coastal waters. The large variations in simulated Chl:C ratios within the SNS, both in a space and time, indicate that ignorance of photoacclimation can lead to potentially flawed estimates for primary production or phytoplankton biomass as was recently pointed out by Arteaga et al. (2014) and Behrenfeld et al. (2015), who used photoacclimation schemes to derive Chl:C ratios at global scales. Here we show that such considerations apply also at coastal environments, which may be critical, given the increasing recognition of the role of coastal-shelf systems in the global carbon and nutrient cycling (Fennel, 2010; Bauer et al., 2013).

Appendix A: Detailed Model Description

A1 Pelagic Module

Local source-sink terms for all dynamic variables, functional description of processes and relationships between quantities and parameters used for the pelagic module are provided in Tab. A1–A3.

Importantly, the biogeochemical model resolves photoacclimation of phytoplankton, described by dynamical partitioning of resources to light harvesting pigments (Eq.A1), enzymes involved in carboxylation reactions (Eq.A1) and nutrient uptake sites (i.e., $f_{LH} + f_C + f_V = 1$) as in Wirtz and Pahlow (2010). Uptake of each nutrient is optimally regulated (as expressed by a_i in Eq.A2–A2), and following Pahlow (2005); Smith et al. (2009), optimality along the affinity-intracellular transport trade-off ($A_i = f_i^A \cdot A_i^*$ and $V_{max,i} = (1 - f_i^A) \cdot V_{max,i}^*$, see Table A3 for the definition of parameters). As a second novelty, the growth model uniquely describes the interdependence between limiting nutrients to be variable between full inter-dependence (as in product rule) and no-interdependence (as in Liebig's law of minimum) as a function of nitrogen quota (See Eq.A2). For a detailed explanation of the phytoplankton growth model and solution of differential expressions in Eq.A1, A1 and A2 refer to Wirtz and Kerimoglu (2016). For enabling the spatial transport of the 'property variables' of phytoplankton such as Q_i, f_{LH} and f_{LH}, they have been transformed to bulk variables by multiplying with the phytoplankton carbon biomass, i.e., B_{C}. Parameterization of the phytoplankton model, except θ_C, fall within the range of values used for the species considered by Wirtz and Kerimoglu (2016). The exact values of the parameters were established by manual tuning, given that important phytoplankton species such as various diatom and dinoflagellate species, and *Phaeocystis* sp. that dominate the phytoplankton composition in the SNS (eg., Wiltshire et al., 2010) have not been studied formerly within the presented model framework.

Phytoplankton losses are due to aggregation and zooplankton grazing (see below). Specific aggregation loss rate (Eq.A2) is described as a function of DOC that mimics transparent exopolymer particles (Schartau et al., 2007) to account for particle stickiness, multiplied by the sum of phytoplankton biomass and of POM reflecting density dependent interaction, which is equivalent to a quadratic loss term. Zooplankton dynamics are described only in terms of their carbon content, assuming stoichiometric homeostasis (Sterner and Elser, 2002). Grazing is described by a Holling Type-3 function of prey concentration (Eq.A2). A lumped loss term accounts for the respiratory losses and exudation of N and P in dissolved inorganic form (Eq.A2),

Biogeosciences Discuss., doi:10.5194/bg-2017-104, 2017
Manuscript under review for journal Biogeosciences
Discussion started: 30 March 2017

which are adjusted depending on the balance between the stoichiometry of zooplankton and that of the ingested food for maintaining the homeostasis (Eq.A2). Effect of the organisms at higher trophic levels, mainly by fish and gelatinous zooplankton are mimicked by a density-dependent mortality of zooplankton, modified by a function of total attenuation of Photosynthetically Available Radiation (PAR) (Eq.A2) to account for higher predation pressure exerted by fish at the off-shore regions of the North Sea, which amounts to about two times that in the coastal regions according to the estimates based on trawl surveys (Maar et al., 2014).

Settling velocity of POM, expressed by w_{POM} is prescribed as a constant value, whereas that of phytoplankton, w_B is assumed to be modified by their nutrient (quota) status. As decreased internal nutrient quotas likely affect the cells ability to regulate buoyancy and lead to faster migration towards deeper, potentially nutrient rich waters (Boyd and Gradmann, 2002), we assume that maximum sinking rates realized at fully depleted quotas approach to a small background value with increasing quotas as has been observed especially for, but not limited to, diatoms (Smayda and Boleyn, 1965; Bienfang and Harrison, 1984).

Finally, all kinetic rates were modified for ambient water temperature, T (K) using the Q10 rule parameterized specifically for autotrophs and small heterotrophs (=bacteria for hydrolysis and remineralization) and for zooplankton.

Table A1. Source-sink terms of the dynamic variables of the pelagic module. The index i represents the elements C, N, P. By definition, $Q_{\mathrm{C}} = Q_{\mathrm{C}}^{Z}$=1, Q_i=B_i/B_{C}. Dynamics of Dissolved Inorganic Carbon (DIC) is not resolved, thus (Eq.A1) not integrated for i=C. Description of processes or functional relationships (capital letters) and of parameters (small letters) are provided in Tables A2 and A3, respectively.

Autotrophic biomass	$s(B_{\mathrm{C}})$	$= (V_{\mathrm{C}} - \sum_i V_i \zeta_i - L_A) \cdot B_{\mathrm{C}} - G \cdot Z_{\mathrm{C}}$	(A1)
Internal quota	$s(Q_i)$	$= V_i - V_{\mathrm{C}} Q_i$	(A2)
Zooplankton	$s(Z_{\mathrm{C}})$	$= (\gamma G - M - L_Z) \cdot Z_{\mathrm{C}}$	(A3)
Dissolved inorganics	$s(\mathrm{DIM}_i)$	$= L_Z Z_{\mathrm{C}} Q_i^Z + r_{\mathrm{DOM}}\,\mathrm{DOM}_i - V_i\, B_{\mathrm{C}}$	(A4)
Dissolved organics	$s(\mathrm{DOM}_i)$	$= r_{\mathrm{POM}}\,\mathrm{POM}_i - r_{\mathrm{DOM}}\mathrm{DOM}_i$	(A5)
Particulate organics	$s(\mathrm{POM}_i)$	$= L_A B_{\mathrm{C}} Q_i + (1-\gamma) G Z_{\mathrm{C}} Q_i + M Z_{\mathrm{C}} Q_i^Z - r_{\mathrm{POM}}\mathrm{POM}_i$	(A6)
Carboxylation (Rub)	$s(f_{\mathrm{C}})$	$= \delta_{\mathrm{C}} \cdot \left(\frac{\partial V_{\mathrm{C}}}{\partial f_{\mathrm{C}}} + \sum_i \frac{\partial V_{\mathrm{C}}}{Q_i} \frac{\mathrm{d}Q_i}{\mathrm{d}f_{\mathrm{C}}} \right)$	(A7)
Pigmentation (Chl)	$s(f_{\mathrm{LH}})$	$= \delta_{\mathrm{LH}} \cdot \left(\frac{\partial V_{\mathrm{C}}}{\partial f_{\mathrm{LH}}} + \sum_i \frac{\partial V_{\mathrm{C}}}{\partial Q_i} \frac{\mathrm{d}Q_i}{\mathrm{d}f_{\mathrm{LH}}} \right)$	(A8)

A2 Benthic Module

The benthic module provides simplistic descriptions of the degradation of N and P from POM to DIM, their fluxes across the benthic-pelagic interface, removal of N due to denitrification and accounts for the sorption dynamics of P.

POM degrades into DIM in one step, described as a first order reaction, the rate of which is modified for temperature using the Q10 rule. POM flux into the sediments by settling of material from the water fuels the benthic POM (bPOM) (Eq.A4). On the other hand, diffusive flux of DIM is possibly bi-directional, depending on the concentration gradient between water

Biogeosciences Discuss., doi:10.5194/bg-2017-104, 2017
Manuscript under review for journal Biogeosciences
Discussion started: 30 March 2017

Table A2. Process descriptions and functional relationships. The index i represents the elements C, N and P. The index j represents groups with different Q10 values. Description of parameters (small letters) are provided in Tab. A3.

Carbon uptake	V_{C}	$= P \cdot g_n\left(\mathcal{C}_n\left(q_{\mathrm{N}}, \mathcal{C}_n\left(q_{\mathrm{P}}, q_{\mathrm{C}}\right)\right)\right) - \sum_i \zeta_i V_i$	(A9)
Light lim. primary prod.	P	$= f_{\mathrm{C}}\, P_{\max} \cdot \left(1 - \mathrm{e}^{-\alpha\theta \mathrm{PAR}/P_{\max}}\right)$	(A10)
Chlorophyll conc. in chloroplasts	θ	$= \theta_{\mathrm{C}} \frac{f_{\mathrm{LH}}}{q_{\mathrm{N}} f_{\mathrm{C}}}$	(A11)
Relative resource availability	q_i	$= \frac{Q_i - Q_i^0}{Q_i^* - Q_i^0}$	(A12)
Co-limitation function	$\mathcal{C}_n(q_i, q_j)$	$= q_i \cdot g_n\left(\frac{q_j}{q_i}\right) \cdot \left(1 + \frac{q_i q_j}{n} + log(4^{-1/n} + 0.5/n)\right)$	(A13)
Queuing function	$g_n(r)$	$= \frac{r - r^{1+n}}{1 - r^{1+n}}$	(A14)
Degree of independence	n	$= n^* \cdot (1 + q_{\mathrm{N}})$	(A15)
Nutrient uptake	V_i	$= f_{\mathrm{V}}\, a_i \cdot \left(V_{\max,i}^{-1} + (A_i \mathrm{DIM}_i)^{-1}\right)^{-1}$	(A16)
Uptake activity	a_i	$= \left(1 + \mathrm{e}^{-\tau_{\mathrm{V}} \frac{\mathrm{d}V_{\mathrm{C}}}{\mathrm{d}a_i}}\right)^{-1}$	(A17)
Flexibility (X =C, LH)	δ_X	$= (f_X - f^{\min}) \cdot (1 - f^{\min} - f_{\mathrm{C}} - f_{\mathrm{LH}})$	(A18)
Losses due to aggregation	L_A	$= L_A^* \cdot \left(\frac{{}^a DOC^{\mathrm{DOM_C}}}{1 + {}^a DOC^{\mathrm{DOM_C}}}\right) \cdot \left(B_{\mathrm{N}} + \mathrm{POM_N}\right)$	(A19)
Grazing	G	$= G_{max} \frac{B_{\mathrm{C}}^2}{K_G^2 + B_{\mathrm{C}}^2}$	(A20)
Zooplankton loss	L_Z	$= m_r Q_i^Z - S +$ max(0,$\gamma G(Q_i - Q_i^Z)$)	(A21)
Zooplankton homeostatic adjustment	S	$=$ if $(m_r Q_i^Z + \gamma G(Q_i - Q_i^Z)) < 0$: $(1-\gamma) G Q_i$; else:0	(A22)
Zooplankton mortality	M_i	$= m_f \cdot \left(1 + \Delta_f \cdot \left(1 - \left(1 + \mathrm{e}^{s_k \cdot (k_{tot}^* - k_{tot})}\right)^{-1}\right)\right) \cdot Z_{\mathrm{C}}$	(A23)
Total PAR attenuation	k_{tot}	$= -\frac{z}{\eta_2} - \int_z^0 \sum_i k_{c,i} c_i(z') dz'$	(A24)
Phytoplankton sinking	w_B	$= w_B^0 + w_B^* \mathrm{e}^{-s_w q_N q_P}$	(A25)
Temperature dependence	F_T^j	$= Q10_j^{(T - T_{\mathrm{ref}}/10)}$	(A26)

and soil (Eq.A4). Inorganic phosphorus (denoted as TIP,(Eq.A4) is assumed to exist in two states: sorbed and dissolved state. Fraction of the sorbed state is given by a function of dissolved oxygen (DO), to account for the production and adsorption of Fe-P complexes in oxic conditions and their desorption at anoxic conditions (Eq.A4). Given the observed inverse relationship between temperature and oxygen concentrations in sediments (eg., Jensen et al., 1995), DO is heuristically estimated as a function of temperature (T) to capture the seasonal hypoxia events. Resulting functional relationships between the sorbed fraction of TIP, T and DO are shown in Fig.A1(a-b). Following the simplistic approach used for the ECOHAM model (Pätsch and Kühn, 2008), denitrification rate is estimated from the degradation rate (Eq.A4) using empirically derived ratios and stoichiometric conversions, considering in addition the limitation imposed by the available DIN and inhibition by DO (Soetaert et al., 1996). Resulting functional relationships between denitrification, T and DO are shown in Fig.A1(c-d).

Biogeosciences Discuss., doi:10.5194/bg-2017-104, 2017
Manuscript under review for journal Biogeosciences
Discussion started: 30 March 2017

Table A3. Parameters of the pelagic module. Codes for sources: c: calibrated; a: assumed; l: typical literature value; d: by definition; 1:Wirtz and Kerimoglu (2016); 2:Hansen et al. (1997, for copepods); 3:Oubelkheir et al. (2005); 4:Stedmon et al. (2001); 5:Maar et al. (2014)

Symbol	Description	Value	Unit	Source
Parameters relevant to phytoplankton				
α	Light absorption coefficient	0.2	m^2 mmolC(µE gCHL)$^{-1}$	1,c
A^*_P	Affinity to PO_4	0.15	m^3(mmolC d)$^{-1}$	1,c
A^*_N	Affinity to inorganic N	0.4	m^3(mmolC d)$^{-1}$	1
P^*_{max}	Potential photosynthesis rate	9.0	d^{-1}	1,c
θ_C	CHL-a/C ratio in chloroplasts	1.0	gChl molC^{-1}	c
Q^0_N	Subsistence quota for N	0.035	molN molC^{-1}	1,c
Q^0_P	Subsistence quota for P	0.0	molP molC^{-1}	1
Q^*_N	Reference N quota	0.17	molN molC^{-1}	1,c
Q^*_P	Reference P quota	0.0055	molP molC^{-1}	1
n^*	specific independence	4.0	-	1,c
$V^0_{max,N}$	Potential N uptake rate	1.0	molN (mmolC d)$^{-1}$	1,c
$V^0_{max,P}$	Potential P uptake rate	0.1	molP (mmolC d)$^{-1}$	1,c
ζ_N	C cost of N assimilation	4.0	molC molN^{-1}	1,c
ζ_P	C cost of P assimilation	24.0	molC molP^{-1}	1,c
τ_v	Relaxation time scale for a_i	10	d	1
f^{min}	Minimum allocation	0.02	-	1
w^*_B	Maximum quota-dependent sinking rate	3.0	m d^{-1}	c
w^0_B	Background sinking rate	0.2	m d^{-1}	c
s_w	Scaling coefficient for sinking function	4.0	-	c
L^*_A	Maximum aggregation rate	0.003	molC molN^{-1}	c
a_{DOC}	DOC specific aggregation coefficient	0.1	mmolC m^{-3}	c
$Q10_B$	Q10 coefficient for autotrophs and bacteria	1.5	-	1

(continued on the next page)

Biogeosciences Discuss., doi:10.5194/bg-2017-104, 2017
Manuscript under review for journal Biogeosciences
Discussion started: 30 March 2017

(continues from the previous page)

Symbol	Description	Value	Unit	Source
Parameters relevant to zooplankton				
Q_N^Z	N:C ratio	0.25	molN molC^{-1}	1
Q_P^Z	P:C ratio	0.02	molP molC^{-1}	1
G_{max}	Max. grazing rate	1.2	d^{-1}	2
γ	Assimilation efficiency	0.35	-	2
K_G	Half saturation constant for grazing	20.0	mmolC m^{-3}	2
m_r	Basal respiration rate	0.02	d^{-1}	1
m_f	Base mortality rate	0.02	m^3 (mmolC d) $^{-1}$	c
Δ_f	Maximum incremental mortality factor	1.0	-	5
k_{tot}^*	Critical total PAR attenuation	0.4	m^2 mmolC^{-1}	c
s_k	Scaling coefficient for mortality function	10.0	mmolC m^{-2}	c
$Q10_Z$	Q10 coefficient for zooplankton	2.0	-	1
Other biogeochemical parameters				
T_{ref}	Reference temperature for kinetic rates	288	K	d
w_{POM}	Sinking rate of POM	6.0	m d^{-1}	c
r_{POM}	Hydrolysis rate	0.03	d^{-1}	c
r_{DOM}	Remineralization rate	0.03	d^{-1}	c
k_B	Attenuation coefficient for phytoplankton	0.015	m^2 mmolC^{-1}	3
k_{POC}	Attenuation coefficient for POC	0.01	m^2 mmolC^{-1}	3
k_{DOC}	Attenuation coefficient for DOC	0.0025	m^2 mmolC^{-1}	4

Biogeosciences Discuss., doi:10.5194/bg-2017-104, 2017
Manuscript under review for journal Biogeosciences
Discussion started: 30 March 2017

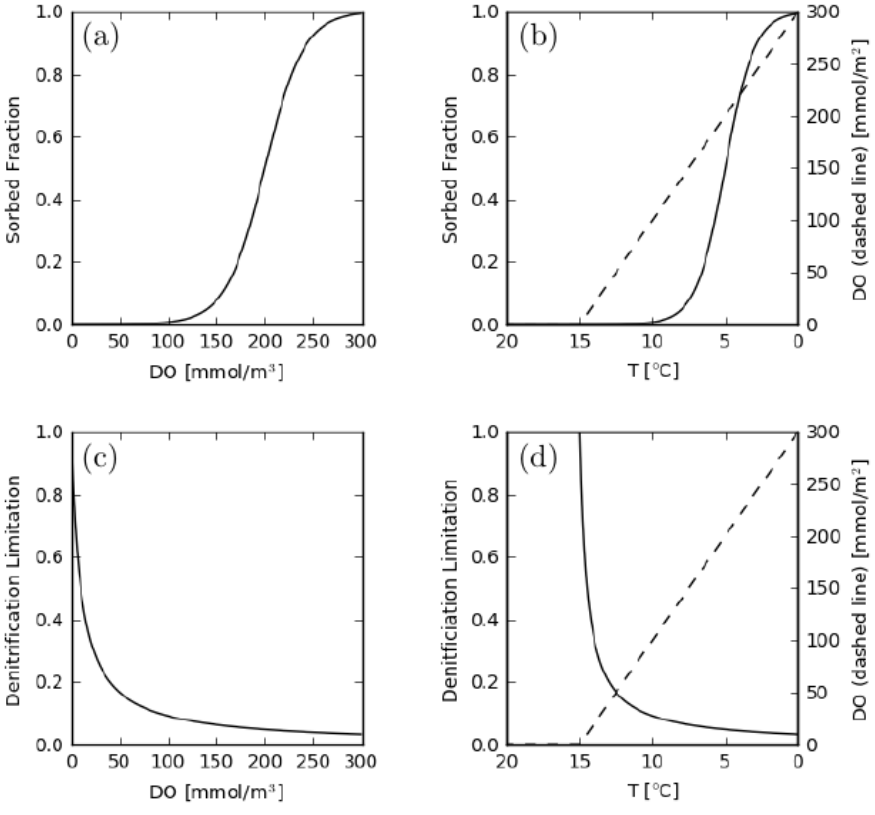

Figure A1. Fraction of sorbed fraction of benthic phosphorus as functions of DO (a) and T (b), regulation of benthic denitrification rate as functions of DO (c) and T (d), and DO as a function of T (b,d).

Biogeosciences Discuss., doi:10.5194/bg-2017-104, 2017
Manuscript under review for journal Biogeosciences
Discussion started: 30 March 2017

Table A4. Source-sink terms of the dynamic variables, and functional relationships of the benthic module. $sDIM_X$=sDIX and $sPOM_X$=sPOX, where X={N,P}. Description of parameters (small letters) are provided in Tab.A5

Dynamics:			
Benthic POM	$s(\text{bPOM}_i)$	$= E_{\text{POM}} - R_{\text{i}}$	
Benthic TIP	$s(\text{bTIP})$	$= E_{\text{DIP}} + R_{\text{P}}$	
Benthic DIN	$s(\text{bDIN})$	$= E_{\text{DIN}} + R_{\text{N}} - \Upsilon$	
Functional relationships:			
Benthic Remineralization rate	R_{i}	$= r_B \cdot \text{sPOM}_{\text{i}}$	(A27)
POM exchange with water	E_{POX}	$= \psi_{POM} * POM$	(A28)
DIM exchange with water	E_{DIX}	$= D_{DIM} \cdot \frac{\text{DIM}-\text{bDIM}}{\Delta_Z}$	(A29)
Fraction of inorganic P in dissolved phase	bDIP	$= 1 - \text{bAP}$	(A30)
Fraction of inorganic P in adsorbed phase	bAP	$= \left(1 + \text{e}^{s_a \cdot (\text{bDO}^* - \text{bDO})}\right)^{-1}$	(A31)
Denitrification	Υ	$= c_{O:N} c_{N:O} R_{\text{N}} \cdot \left(\frac{\text{bDIN}}{K_{\Upsilon,DIN} + \text{bDIN}}\right) \cdot \left(1 - \frac{\text{bDO}}{K_{\Upsilon,DO} + \text{bDO}}\right)$	(A32)
Benthic dissolved oxygen	bDO	$= 300.0 - c_{DO} * T$	(A33)
Temperature dependence	F_T^b	$= Q10_b^{(T - T_{\text{ref}}/10.0)}$	(A34)

Table A5. Parameters of the benthic module. Codes for sources: c:calibrated; a:assumed; l: typical literature value; 1:Soetaert et al. (1996); 2:Seitzinger and Giblin (1996)

Symbol	Description	Value	Unit	Source
r_b	Benthic degradation rate	0.05	d^{-1}	c
ψ_{POM}	Sinking velocity of POM across the benthic-pelagic interface	3.0	d^{-1}	c
D_{DIM}	Diffusivity of DIM across the benthic-pelagic interface	5e-4	$\text{m}^2\ \text{d}^{-1}$	l
Δ_Z	Thickness of the boundary layer	0.2	m	a
c_{DO}	DO-T coefficient	20	mmolO K^{-1}	c
$K_{\Upsilon,DO}$	Half saturation for DO inhibition of denitrification	10	mmolO m^{-2}	l
$K_{\Upsilon,DIN}$	Half saturation for DIN limitation of denitrification	30	mmolO m^{-2}	l
$c_{O:N}$	Consumed oxygen per degraded nitrogen	6.625	molO molN^{-3}	a
$c_{N:O}$	Denitrified N per consumed oxygen	0.116	molN molO^{-3}	2
s_a	Scaling coefficient for DO-sorption relationship	0.05	$\text{m}^3\ \text{mmolC}^{-1}$	c
bDO^*	Critical benthic DO concentration for P-soprtion	200	molO m^{-3}	c
$Q10_b$	Q10 coefficient for benthic reactions	2.0	-	l

Author contributions. OK and KW designed and outlined the study. OK calibrated the model, ran the simulations, performed the majority of analyses and drafted the manuscript. OK and RH created the model setup and prepared model forcing. KW, RH and OK developed the biogeochemical model and wrote the model code. RH prepared the salinity cruise plot. JM and RH handled the Scanfish data and contributed to the preperation of Scanfish plot. JM developed a SPM climatology for a former model version. All authors participated in revising the manuscript.

Acknowledgements. We gratefully acknowledge Markus Schartau (Helmholtz Centre for Ocean Research Kiel) for his contributions to the initial development of MAECS, Carsten Lemmen (HZG) for his help with setting up the supercomputing environment, Sonja van Leeuwen (Centre for Environment, Fisheries and Aquaculture Science) for providing data on riverine fluxes, S"ønke Hohn (Leibniz Centre for Tropical Marine Research) and Annika Eisele (HZG) for their assistance in formatting and checking the river data, Fabian Große (University of Hamburg -UH) and Markus Kreus (UH) for providing the boundary conditions for the biogeochemical model and Johannes Pätsch (UH) for providing the SPM climatology. Justus van Beusekom (based on his work in AWI, now HZG), Karen H. Wiltshire (AWI), Annika Grage (NLWKN), Thorkild Petenati (LLUR), Sieglinde Weigelt-Krenz (BSH) are acknowledged for providing monitoring data. Justus van Beusekom (HZG), Fabian Große (UH), Ivan Kuznetsov (HZG), Hermann-Josef Lenhart (UH) and Corinna Schrum (HZG) are acknowledged for their helpful comments during various stages of this work. This is a contribution by the Helmholtz Society through the PACES program. OK, RH and KW were supported by the German Federal Ministry of Education and Research (BMBF) throgh the MOSSCO project. OK and KW were additionally supported by the German Research Foundation (DFG) through the priority program 1704 Dynatrait. The authors gratefully acknowledge the computing time granted by the John von Neumann Institute for Computing (NIC) and provided on the supercomputer JURECA (Jülich Supercomputing Centre, 2016) at Jülich Supercomputing Centre.

References

Alvarez-Fernandez, S. and Riegman, R.: Chlorophyll in North Sea coastal and offshore waters does not reflect long term trends of phytoplankton biomass, Journal of Sea Research, 91, 35–44, doi:10.1016/j.seares.2014.04.005, 2014.

Alvarez-Fernandez, S., Lindeboom, H., and Meesters, E.: Temporal changes in plankton of the North Sea: Community shifts and environmental drivers, Marine Ecology Progress Series, 462, 21–38, doi:10.3354/meps09817, 2012.

Amann, T., Weiss, A., and Hartmann, J.: Carbon dynamics in the freshwater part of the Elbe estuary, Germany: Implications of improving water quality, Estuarine, Coastal and Shelf Science, 107, 112–121, doi:10.1016/j.ecss.2012.05.012, 2012.

Arteaga, L., Pahlow, M., and Oschlies, A.: Global patterns of phytoplankton nutrient and light colimitation inferred from an optimality-based model, Global Biogeochemical Cycles, 28, 648–661, doi:10.1002/2013GB004668, 2014.

Baschek, B., Schroeder, F., Brix, H., Riethmüller, R., Badewien, T. H., Breitbach, G., Brügge, B., Colijn, F., Doerffer, R., Eschenbach, C., Friedrich, J., Fischer, P., Garthe, S., Horstmann, J., Krasemann, H., Metfies, K., Ohle, N., Petersen, W., Pröfrock, D., Röttgers, R., Schlüter, M., Schulz, J., Schulz-Stellenfleth, J., Stanev, E., Winter, C., Wirtz, K., Wollschläger, J., Zielinski, O., and Ziemer, F.: The Coastal Observing System for Northern and Arctic Seas (COSYNA), Ocean Science Discussions, pp. 1–73, doi:10.5194/os-2016-31, 2016.

Bauer, J. E., Cai, W.-J., Raymond, P. A., Bianchi, T. S., Hopkinson, C. S., and Regnier, P. A. G.: The changing carbon cycle of the coastal ocean., Nature, 504, 61–70, doi:10.1038/nature12857, 2013.

Beaugrand, G., Harlay, X., and Edwards, M.: Detecting plankton shifts in the North Sea: A new abrupt ecosystem shift between 1996 and 2003, Marine Ecology Progress Series, 502, 85–104, doi:10.3354/meps10693, 2014.

Behrenfeld, M. J., O'Malley, R. T., Boss, E. S., Westberry, T. K., Graff, J. R., Halsey, K. H., Milligan, A. J., Siegel, D. A., and Brown, M. B.: Revaluating ocean warming impacts on global phytoplankton, Nature Climate Change, 6, 1–27, doi:10.1038/nclimate2838, 2015.

Bienfang, P. and Harrison, P.: CO-variation of sinking rate and cell quota among nutrient replete marine phytoplankton, Marine Ecology Progress Series, 14, 297–300, 1984.

Blackford, J., Allen, J., and Gilbert, F.: Ecosystem dynamics at six contrasting sites: a generic modelling study, Journal of Marine Systems, 52, 191–215, doi:10.1016/j.jmarsys.2004.02.004, 2004.

Bonachela, J. A., Allison, S. D., Martiny, A. C., and Levin, S. A.: A model for variable phytoplankton stoichiometry based on cell protein regulation, Biogeosciences, 10, 4341–4356, doi:10.5194/bg-10-4341-2013, 2013.

Bonachela, J. A., Klausmeier, C. A., Edwards, K. F., Litchman, E., and Levin, S. A.: The role of phytoplankton diversity in the emergent oceanic stoichiometry, Journal of Plankton Research, 38, 1021–1035, doi:10.1093/plankt/fbv087, 2016.

Boyd, C. and Gradmann, D.: Impact of osmolytes on buoyancy of marine phytoplankton, Marine Biology, 141, 605–618, doi:10.1007/s00227-002-0872-z, 2002.

Brockmann, U., Raabe, T., Hesse, K., Viehweger, K., Rick, S., Starke, A., Fabiszisky, B., Topçu, D., and Heller, R.: Seasonal budgets of the nutrient elements N and P at the surface of the German Bight during winter 1996, spring 1995, and summer 1994, Deutsche Hydrographische Zeitschrift, 51, 267–291, doi:10.1007/bf02764177, 1999.

Brockmann, U. H.: Organic matter in the Elbe estuary, Netherlands Journal of Aquatic Ecology, 28, 371–381, doi:10.1007/BF02334207, 1994.

Bruggeman, J. and Bolding, K.: A general framework for aquatic biogeochemical models, Environmental Modelling & Software, 61, 249–265, doi:10.1016/j.envsoft.2014.04.002, 2014.

Burchard, H. and Bolding, K.: GETM: A general estuarine transport model, Tech. rep., Joint Research Centre, Ispra, Italy, 2002.

Burchard, H., Bolding, K., Kühn, W., Meister, A., Neumann, T., and Umlauf, L.: Description of a flexible and extendable physical-biogeochemical model system for the water column, Journal of Marine Systems, 61, 180–211, doi:10.1016/j.jmarsys.2005.04.011, 2006.

Burchard, H., Flöser, G., Staneva, J. V., Badewien, T. H., and Riethmüller, R.: Impact of Density Gradients on Net Sediment Transport into the Wadden Sea, Journal of Physical Oceanography, 38, 566–587, doi:10.1175/2007JPO3796.1, 2008.

Cloern, J. E., Foster, S. Q., and Kleckner, A. E.: Phytoplankton primary production in the world's estuarine-coastal ecosystems, Biogeosciences, 11, 2477–2501, doi:10.5194/bg-11-2477-2014, 2014.

Daewel, U. and Schrum, C.: Simulating long-term dynamics of the coupled North Sea and Baltic Sea ecosystem with ECOSMO II: Model description and validation, Journal of Marine Systems, 119-120, 30–49, doi:10.1016/j.jmarsys.2013.03.008, 2013.

Dähnke, K., Bahlmann, E., and Emeis, K.: A nitrate sink in estuaries? An assessment by means of stable nitrate isotopes in the Elbe estuary, Limnology and Oceanography, 53, 1504–1511, doi:10.4319/lo.2008.53.4.1504, 2008.

Daines, S. J., Clark, J. R., and Lenton, T. M.: Multiple environmental controls on phytoplankton growth strategies determine adaptive responses of the N : P ratio, Ecology Letters, 17, 414–425, doi:10.1111/ele.12239, 2014.

de Mora, L., Butenschön, M., and I., A. J.: How should sparse marine in situ measurements be compared to a continuous model: an example, Geoscientific Model Development, 6, 533–548, doi:10.5194/gmd-6-533-2013, 2013.

Durham, W. M. and Stocker, R.: Thin phytoplankton layers: characteristics, mechanisms, and consequences, Annual Review of Marine Science, 4, 177–207, doi:10.1146/annurev-marine-120710-100957, 2012.

Ebenhöh, W.: Shallowness may be a major factor generating nutrient gradients in the Wadden Sea, Ecological Modelling, 174, 241–252, doi:10.1016/j.ecolmodel.2003.07.011, 2004.

Emeis, K. C., van Beusekom, J., Callies, U., Ebinghaus, R., Kannen, A., Kraus, G., Kröncke, I., Lenhart, H., Lorkowski, I., Matthias, V., Möllmann, C., Pätsch, J., Scharfe, M., Thomas, H., Weisse, R., and Zorita, E.: The North Sea - A shelf sea in the Anthropocene, Journal of Marine Systems, 141, 18–33, doi:10.1016/j.jmarsys.2014.03.012, 2015.

Fennel, K.: The role of continental shelves in nitrogen and carbon cycling: Northwestern North Atlantic case study, Ocean Science, 6, 539–548, doi:10.5194/os-6-539-2010, 2010.

Fennel, K., Wilkin, J., Levin, J., Moisan, J., O'Reilly, J., and Haidvogel, D.: Nitrogen cycling in the Middle Atlantic Bight: Results from a three-dimensional model and implications for the North Atlantic nitrogen budget, Global Biogeochemical Cycles, 20, 1–14, doi:10.1029/2005GB002456, 2006.

Fernand, L., Weston, K., Morris, T., Greenwood, N., Brown, J., and Jickells, T.: The contribution of the deep chlorophyll maximum to primary production in a seasonally stratified shelf sea, the North Sea, Biogeochemistry, 113, 153–166, doi:10.1007/s10533-013-9831-7, 2013.

Flöser, G., Burchard, H., and Riethmüller, R.: Observational evidence for estuarine circulation in the German Wadden Sea, Continental Shelf Research, 31, 1633–1639, doi:http://dx.doi.org/10.1016/j.csr.2011.03.014, 2011.

Ford, D. A., van der Molen, J., Hyder, K., Bacon, J., Barciela, R., Creach, V., McEwan, R., Ruardij, P., and Forster, R.: Observing and modelling phytoplankton community structure in the North Sea: can ERSEM-type models simulate biodiversity?, Biogeosciences Discussions, 2016, 1–39, doi:10.5194/bg-2016-304, 2016.

Freund, J. A., Grüner, N., Brüse, S., and Wiltshire, K. H.: Changes in the phytoplankton community at Helgoland, North Sea: lessons from single spot time series analyses, Marine Biology, 159, 2561–2571, doi:10.1007/s00227-012-2013-7, 2012.

Geider, R., MacIntyre, H., and Kana, T.: Dynamic model of phytoplankton growth and acclimation: responses of the balanced growth rate and the chlorophyll a:carbon ratio to light, nutrient-limitation and temperature, Marine Ecology Progress Series, 148, 187–200, 1997.

Geyer, B.: High-resolution atmospheric reconstruction for Europe 1948–2012: coastDat2, Earth System Science Data, 6, 147–164, doi:doi:10.5194/essd-6-147-2014, 2014.

Grant, M., Jackson, T., Chuprin, A., Sathyendranath, S., Zühlke, M., Storm, T., Boettcher, M., and Fomferra, N.: OC-CCI v2.0 Product User Guide 2.0.5, Tech. rep., ESA, 2015.

Gröger, M., Maier-Reimer, E., Mikolajewicz, U., Moll, A., and Sein, D.: NW European shelf under climate warming: implications for open ocean – shelf exchange, primary production, and carbon absorption, Biogeosciences, 10, 3767–3792, doi:10.5194/bg-10-3767-2013, 2013.

Große, F., Greenwood, N., Kreus, M., Lenhart, H. J., Machoczek, D., Pätsch, J., Salt, L. A., and Thomas, H.: Looking beyond stratification: a model-based analysis of the biological drivers of oxygen depletion in the North Sea, Biogeosciences, 13, 2511–2535, doi:10.5194/bgd-12-12543-2015, 2016.

Grunwald, M., Dellwig, O., Kohlmeier, C., Kowalski, N., Beck, M., Badewien, T. H., Kotzur, S., Liebezeit, G., and Brumsack, H.-J.: Nutrient dynamics in a back barrier tidal basin of the Southern North Sea: Time-series, model simulations, and budget estimates, Journal of Sea Research, 64, 199–212, doi:10.1016/j.seares.2010.02.008, 2010.

Hansen, P., Bjørnsen, P., and Hansen, B.: Zooplankton grazing and growth: Scaling within the 2-2,000 μm body size range, Limnology and Oceanography, 42, 687–704, 1997.

Heath, M. R., Edwards, A. C., Patsch, J., and Turrell, W.: Modelling the behaviour of nutrient in the coastal waters of Scotland, Tech. rep., Scottish Executive Central Research Unit,, Edinburgh, 2002.

Hetzel, Y., Pattiaratchi, C., Lowe, R., and Hofmeister, R.: Wind and tidal mixing controls on stratification and dense water outflows in a large hypersaline bay, Journal of Geophysical Research: Oceans, 120, 6034–6056, doi:10.1002/2015JC010733, 2015.

Hofmeister, R., Bolding, K., Hetland, R. D., Schernewski, G., Siegel, H., and Burchard, H.: The dynamics of cooling water discharge in a shallow, non-tidal embayment, Continental Shelf Research, 71, 68–77, doi:10.1016/j.csr.2013.10.006, 2013.

Hofmeister, R., Flöser, G., and Schartau, M.: Estuary-type circulation as a factor sustaining horizontal nutrient gradients in freshwater-influenced coastal systems, Geo-Marine Letters, doi:10.1007/s00367-016-0469-z, 2016.

Holt, J. and Umlauf, L.: Modelling the tidal mixing fronts and seasonal stratification of the Northwest European Continental shelf, Continental Shelf Research, 28, 887–903, doi:10.1016/j.csr.2008.01.012, 2008.

Hydes, D. J., Le Gall, A. C., and Proctor, R.: The balance of supply of nutrients and demands of biological production and denitrification in a temperate latitude shelf sea — a treatment of the southern North Sea as an extended estuary, Marine Chemistry, 68, 117–131, 1999.

Jensen, H. S., Mortensen, P. B., Andersen, F. O., Rasmussen, E., and Jensen, A.: Phosphorus cycling in a coastal marine sediment, Aarhus Bay, Denmark, Limnology and Oceanography, 40, 908–917, 1995.

Jolliff, J., Kindle, J., Shulman, I., Penta, B., Friedrichs, M., Helber, R., and Arnone, R.: Summary diagrams for coupled hydrodynamic-ecosystem model skill assessment, Journal of Marine Systems, 76, 64–82, doi:10.1016/j.jmarsys.2008.05.014, 2009.

Jülich Supercomputing Centre: JURECA: General-purpose supercomputer at Jülich Supercomputing Centre, Journal of large-scale research facilities, 2, doi:10.17815/jlsrf-2-121, 2016.

Klausmeier, C., Litchman, E., Daufresne, T., and Levin, S.: Optimal nitrogen-to-phosphorus stoichiometry of phytoplankton, Nature, 429, 171–174, doi:1.1029/2001GL014649, 2004.

Litchman, E., Pinto, P. D. T., Klausmeier, C. A., Thomas, M. K., and Yoshiyama, K.: Linking traits to species diversity and community structure in phytoplankton, Hydrolobiologia, 653, 15–28, doi:10.1007/s10750-010-0341-5, 2010.

Llewellyn, C. A., Fishwick, J. R., and Blackford, J. C.: Phytoplankton community assemblage in the English Channel : a comparison using chlorophyll a derived from HPLC-CHEMTAX and carbon derived from microscopy cell counts, Journal of Plankton Research, 27, 103–119, doi:10.1093/plankt/fbh158, 2005.

Löder, M., Kraberg, A., Aberle, N., Peters, S., and Wiltshire, K.: Dinoflagellates and ciliates at Helgoland Roads, North Sea, Helgoland Marine Research, 66, 11–23, doi:10.1007/s10152-010-0242-z, 2012.

Loebl, M., Dolch, T., and van Beusekom, J. E. E.: Annual dynamics of pelagic primary production and respiration in a shallow coastal basin, Journal of Sea Research, 58, 269 – 282, doi:10.1016/j.seares.2007.06.003, 2007.

Loebl, M., Colijn, F., van Beusekom, J. E. E., Baretta-Bekker, J. G., Lancelot, C., Philippart, C. J. M., Rousseau, V., and Wiltshire, K. H.: Recent patterns in potential phytoplankton limitation along the Northwest European continental coast, Journal of Sea Research, 61, 34–43, doi:10.1016/j.seares.2008.10.002, 2009.

Los, F. J., Villars, M. T., and van der Tol, M. W. M.: A 3-dimensional primary production model (BLOOM/GEM) and its applications to the (southern) North Sea (coupled physical–chemical–ecological model), Journal of Marine Systems, 74, 259–294, doi:10.1016/j.jmarsys.2008.01.002, 2008.

Maar, M., Rindorf, A., Møller, E. F., Christensen, A., Madsen, K. S., and van Deurs, M.: Zooplankton mortality in 3D ecosystem modelling considering variable spatial–temporal fish consumptions in the North Sea, Progress in Oceanography, 124, 78–91, doi:10.1016/j.pocean.2014.03.002, 2014.

Maerz, J., Verney, R., Wirtz, K. W., and Feudel, U.: Modeling flocculation processes: Intercomparison of a size class-based model and a distribution-based model, Continental Shelf Research, 31, 84–93, doi:10.1016/j.csr.2010.05.011, 2011.

Maerz, J., Hofmeister, R., van der Lee, E. M., Gräwe, U., Riethmüller, R., and Wirtz, K. W.: Maximum sinking velocities of suspended particulate matter in a coastal transition zone, Biogeosciences, 13, 4863–4876, doi:10.5194/bg-13-4863-2016, 2016.

Meyer, E. M., Pohlmann, T., and Weisse, R.: Thermodynamic variability and change in the North Sea (1948–2007) derived from a multi-decadal hindcast, Journal of Marine Systems, 86, 35–44, doi:10.1016/j.jmarsys.2011.02.001, 2011.

Oubelkheir, K., Sciandra, A., and Babin, M.: Bio-optical and biogeochemical properties of different trophic regimes in oceanic waters, Limnology and Oceanography, 50, 1795–1809, 2005.

Pahlow, M.: Linking chlorophyll – nutrient dynamics to the Redfield N : C ratio with a model of optimal phytoplankton growth, Marine Ecology Progress Series, 287, 33–43, 2005.

Pahlow, M. and Oschlies, A.: Chain model of phytoplankton P, N and light colimitation, Marine Ecology Progress Series, 376, 69–83, doi:10.3354/meps07748, 2009.

Pätsch, J. and Kühn, W.: Nitrogen and carbon cycling in the North Sea and exchange with the North Atlantic—A model study. Part I. Nitrogen budget and fluxes, Continental Shelf Research, 28, 767–787, doi:10.1016/j.csr.2007.12.013, 2008.

Pätsch, J. and Lenhart, H.: Daily Loads of Nutrients, Total Alkalinity, Dissolved Inorganic Carbon and Dissolved Organic Carbon of the European Continental Rivers for the Years 1977-2009, Tech. rep., 2011.

Paulson, C. and Simpson, J.: Irradience measurements in the upper ocean, Journal of Physical Oceanography, 7, 952–956, 1977.

Petersen, W.: FerryBox systems: State-of-the-art in Europe and future development, Journal of Marine Systems, 140, 4–12, doi:10.1016/j.jmarsys.2014.07.003, 2014.

Postma, H.: Transport and accumulation of suspended matter in the Dutch Wadden Sea, Netherlands Journal of Sea Research, 1, 148–180, doi:10.1016/0077-7579(61)90004-7, 1961.

Puls, W., Heinrich, H., and Mayerj, B.: Suspended Particulate Matter Budget for the German Bight, Marine Pollution Bulletin, 34, 398–409, 1997.

Radach, G. and Moll, A.: Review of three-dimensional ecological modeling related to the North Sea shelf system. Part II: Model validation and data needs, Oceanography and Marine Biology, Annual Review, 44, 1–60, 2006.

Radach, G. and Pätsch, J.: Variability of Continental Riverine Freshwater and Nutrient Inputs into the North Sea for the Years 1977 – 2000 and Its Consequences for the Assessment of Eutrophication, Estuaries and Coasts, 30, 66–81, 2007.

Schartau, M., Engel, A., Schröter, J., Thoms, S., Völker, C., and Wolf-Gladrow, D.: Modelling carbon overconsumption and the formation of extracellular particulate organic carbon, Biogeosciences, 4, 13–67, doi:10.5194/bgd-4-13-2007, 2007.

Schrum, C., Siegismund, F., and St. John, M.: Decadal variations in the stratification and circulation patterns of the North Sea. Are the 1990s unusual?, ICES Marine Science Symposia, 219, 121–131, 2003.

Seitzinger, S. P. and Giblin, A. E.: Estimating denitrification in North Atlantic continental shelf sediments, Biogeochemistry, 35, 235–260, 1996.

Smayda, T. J. and Boleyn, B. J.: Experimental observations on the flotation of marine diatoms. 1.Thalassiosira cf. nana, Thalassiosira rotula and Nitzchia seriata, Limnology and Oceanography, 10, 499–509, doi:10.4319/lo.1965.10.4.0499, 1965.

Smith, S. L., Yamanaka, Y., Pahlow, M., and Oschlies, A.: Optimal uptake kinetics: physiological acclimation explains the pattern of nitrate uptake by phytoplankton in the ocean, Marine Ecology Progress Series, 384, 1–12, doi:10.3354/meps08022, 2009.

Smith, S. L., Pahlow, M., Merico, A., and Wirtz, K. W.: Optimality-based modeling of planktonic organisms, Limnology and Oceanography, 56, 2080–2094, doi:10.4319/lo.2011.56.6.2080, 2011.

Soetaert, K., J., H. P. M., and Middelburg, J. J.: A model of early diagenetic processes from the shelf to abyssal depths, Geochimica et Cosmochimica Acta, 60, 1019–1040, 1996.

Stedmon, C., Markager, S., and Kaas, H.: The optics of chromophoric dissolved organic matter (CDOM) in the Greenland Sea: An algorithm for differentiation between marine and terrestrially derived organic matter, Limnology and Oceanography, 46, 2087–2093, 2001.

Sterner, R. and Elser, J.: Ecological stoichiometry: The biology of elements from molecules to the biosphere, Princeton University Press, Princeton, NJ, 2002.

Stips, A., Bolding, K., Pohlmann, T., and Burchard, H.: Simulating the temporal and spatial dynamics of the North Sea using the new model GETM (general estuarine transport model), Ocean Dynamics, 54, 266–283, doi:10.1007/s10236-003-0077-0, 2004.

Su, J., Tian, T., Krasemann, H., Schartau, M., and Wirtz, K.: Response patterns of phytoplankton growth to variations in resuspension in the German Bight revealed by daily MERIS data in 2003 and 2004, Oceanologia, 57, 328–341, doi:10.1016/j.oceano.2015.06.001, 2015.

Tian, T., Merico, A., Su, J., Staneva, J., Wiltshire, K. H., and Wirtz, K. W.: Importance of resuspended sediment dynamics for the phytoplankton spring bloom in a coastal marine ecosystem, Journal of Sea Research, 62, 214–228, 2009.

van Beusekom, J., Brockmann, U., Hesse, K.-J., Hickel, W., Poremba, K., and Tillmann, U.: The importance of sediments in the transformation and turnover of nutrients and organic matter in the Wadden Sea and German Bight, Deutsche Hydrographische Zeitschrift, 51, 245–266, doi:10.1007/BF02764176, 1999.

van Beusekom, J. E. and de Jonge, V. N.: Long-term changes in Wadden Sea nutrient cycles: importance of organic matter import from the North Sea, Hydrobiologia, 475/476, 185–194, 2002.

van Beusekom, J. E., Loebl, M., and Martens, P.: Distant riverine nutrient supply and local temperature drive the long-term phytoplankton development in a temperate coastal basin, Journal of Sea Research, 61, 26–33, doi:10.1016/j.seares.2008.06.005, 2009.

van Leeuwen, S., Tett, P., Mills, D., and van der Molen, J.: Stratified and nonstratified areas in the North Sea: Long-term variability and biological and policy implications Sonja, Journal of Geophysical Research: Oceans, 120, 4670–4686, doi:10.1002/2014JC010485, 2015.

van Leeuwen, S. M., van der Molen, J., Ruardij, P., Fernand, L., and Jickells, T.: Modelling the contribution of deep chlorophyll maxima to annual primary production in the North Sea, Biogeochemistry, 113, 137–152, doi:10.1007/s10533-012-9704-5, 2013.

Weisse, R., Bisling, P., Gaslikova, L., Geyer, B., Groll, N., Hortamani, M., Matthias, V., Maneke, M., Meinke, I., Meyer, E. M. I., Schwichtenberg, F., Stempinski, F., Wiese, F., and Wöckner-Kluwe, K.: Climate services for marine applications in Europe, Earth Perspectives, 2, 1–14, doi:10.1186/s40322-015-0029-0, 2015.

Weston, K., Fernand, L., Mills, D. K., Delahunty, R., and Brown, J.: Primary production in the deep chlorophyll maximum of the central North Sea, Journal of Plankton Research, 27, 909–922, doi:10.1093/plankt/fbi064, 2005.

Wiltshire, K. H., Malzahn, A. M., Wirtz, K. W., Greve, W., Janisch, S., Mangelsdorf, P., Manly, B. F. J., and Boersma, M.: Resilience of North Sea phytoplankton spring bloom dynamics: An analysis of long-term data at Helgoland Roads, Limnology and Oceanography, 53, 1294–1302, doi:10.4319/lo.2008.53.4.1294, 2008.

Wiltshire, K. H., Kraberg, A., Bartsch, I., Boersma, M., Franke, H.-D., Freund, J., Gebühr, C., Gerdts, G., Stockmann, K., and Wichels, A.: Helgoland Roads, North Sea: 45 Years of Change, Estuaries and Coasts, 33, 295–310, doi:10.1007/s12237-009-9228-y, 2010.

Wirtz, K. W. and Kerimoglu, O.: Optimality and variable co-limitation controls autotrophic stoichiometry, Frontiers in Ecology and Evolution, doi:10.3389/fevo.2016.00131, 2016.

Wirtz, K. W. and Pahlow, M.: Dynamic chlorophyll and nitrogen:carbon regulation in algae optimizes instantaneous growth rate, Marine Ecology Progress Series, 402, 81–96, doi:10.3354/meps08333, 2010.

Wollschläger, J., Wiltshire, K. H., Petersen, W., and Metfies, K.: Analysis of phytoplankton distribution and community structure in the German Bight with respect to the different size classes, Journal of Sea Research, 99, 83–96, doi:10.1016/j.seares.2015.02.005, 2015.